Available online at www.sciencedirect.com
SCIENCE DIRECT
Geochimica et Cosmochimica Acta 70 (2006) 3743–3761
Geochimica
www.elsevier.com/locate/gca

U–Pb, Hf and O isotope evidence for two episodes of fluid-assisted zircon growth in marble-hosted eclogites from the Dabie orogen

Yuan-Bao Wu [a,b,e], Yong-Fei Zheng [a,d,*], Zi-Fu Zhao [a,c], Bing Gong [a], Xiaoming Liu [c], Fu-Yuan Wu [d]

[a] CAS Key Laboratory of Crust-Mantle Materials and Environments, School of Earth and Space Sciences, University of Science and Technology of China, Hefei 230026, China
[b] Beijing SHRIMP Center, Chinese Academy of Geological Sciences, Beijing 100037, China
[c] MOE Key Laboratory of Continental Dynamics, Department of Geology, Northwest University, Xi'an 710069, China
[d] State Kay Laboratory of Lithosphere Evolution, Institute of Geology and Geophysics, Chinese Academy of Sciences, Beijing 100029, China
[e] Faculty of Earth Sciences, China University of Geosciences, Wuhan 430074, China

Received 4 January 2006; accepted in revised form 18 May 2006

Abstract

A combined study of internal structure, U–Pb age, and Hf and O isotopes was carried out for metamorphic zircons from ultrahigh-pressure eclogite boudins enclosed in marbles from the Dabie orogen in China. CL imaging identifies two types of zircon that are metamorphically new growth and recrystallized domain, respectively. The metamorphic zircons have low Th and U contents with low Th/U ratios, yielding two groups of $^{206}Pb/^{238}U$ age at 245 ± 3 to 240 ± 2 Ma and 226 ± 4 to 223 ± 2 Ma, respectively. Anomalously high $\delta^{18}O$ values were obtained for refractory minerals, with 9.9 to 21.4‰ for garnet and 16.9‰ for zircon. This indicates that eclogite protolith is sedimentary rocks capable of liberating aqueous fluid for zircon growth during continental subduction-zone metamorphism. Most of the zircons are characterized by very low $^{176}Lu/^{177}Hf$ ratios of 0.000001–0.000028, indicating their growth in association with garnet recrystallization. A few of them falling within the older age group have comparatively high $^{176}Lu/^{177}Hf$ ratios of 0.000192–0.000383, suggesting their growth prior to the formation of garnet in the late stage of subduction. The variations in the Lu/Hf ratios for zircons can thus be used to correlate with garnet growth during eclogite-facies metamorphism. In either case, the zircons have variable $\varepsilon_{Hf}(t)$ values for individual samples, suggesting that their protolith is heterogeneous in Hf isotope composition with localized fluid availability in the bulk processes of orogenic cycle. Nevertheless, a positive correlation exists between $^{206}Pb/^{238}U$ ages and Lu–Hf isotope ratios for the metamorphically recrystallized zircons, suggesting that eclogite-facies metamorphism in the presence of fluid has the identical effect on zircon Lu–Hf and U–Th–Pb isotopic systems. We conclude that the zircons of the older group grew in the presence of fluid during the subduction prior to the onset of peak ultrahigh-pressure metamorphism, whereas the younger zircons grew in the presence of fluid released during the initial exhumation toward high-pressure eclogite-facies regime.

1. Introduction

Fluid, despite a minor component of the continental crust, is very important in controlling a wide spectrum of subduction-zone processes: high-pressure (HP) and ultrahigh-pressure (UHP) metamorphism, and syn-subduction and syn-exhumation magmatism. Metamorphic fluid involved in continental collision has bearing on the deep circulation of surface water, the fate of deeply subducted slab, retrograde alteration and quartz veining (Rumble et al., 2003; Zheng et al., 2003; Li et al., 2004). While the absence of aqueous fluids has been recognized to play a critical role

* Corresponding author. Fax: +86 551 3603554.
E-mail address: yfzheng@ustc.edu.cn (Y.-F. Zheng).

0016-7037/$ - see front matter © 2006 Elsevier Inc. All rights reserved.
doi:10.1016/j.gca.2006.05.011

in preserving UHP metamorphic signatures acquired during deep subduction of continental crust (Liou et al., 1996; Zhang et al., 2003), difficulties were encountered in dating of mineral growth during eclogite-facies metamorphism (e.g., Mork and Mearns, 1986; Brueckner et al., 1996; Zheng et al., 2002). Zircon is one of the most important minerals in U–Pb isotopic geochronology, but its applicability critically depends on contemporaneous growth in response to a given tectonothermal event (Williams et al., 1996). Metamorphic dehydration and anatexis of subducted sediments and hydrothermally altered crust are vital to growth of metamorphic and igneous zircons (Rubatto and Hermann, 2003). Thus the zircon U–Pb geochronology can provide an important means to date fluid-mediated processes during subduction and exhumation of continental crust.

In the past decade, zircon U–Pb dates have been obtained for UHP metamorphic rocks from the Dabie-Sulu orogenic belt in China to constrain their metamorphic and protolith ages (e.g., Ames et al., 1996; Hacker et al., 1998; Ayers et al., 2002; Li et al., 2004; Liu et al., 2004a,b; Zheng et al., 2004, 2005a). However, exact timing of peak UHP metamorphism is controversial, arguably at sometime between 245 and 215 Ma. It is known that metamorphic zircon can form in different stages during subduction-zone metamorphism, such as prograde phase (Vavra et al., 1996; Liati and Gebauer, 1999; Rubatto et al., 1999; Zheng et al., 2005a), peak phase (Gebauer et al., 1997; Hacker et al., 1998; Hermann et al., 2001; Ayers et al., 2002; Rubatto, 2002; Liu et al., 2004a,b), and retrograde phase (Fraser et al., 1997; Roberts and Finger, 1997; Hacker et al., 1998; Ayers et al., 2002; Whitehouse and Platt, 2003; Gray et al., 2004; Liu et al., 2004a,b; Timmermann et al., 2004; Zheng et al., 2005a). Its formation mechanism includes not only new zircon growth (by decomposition or recrystallization of rock-forming minerals with release of zirconium) but also solid-state or anatectic recrystallization of older zircons. Therefore, it is very important to constrain the metamorphic conditions and fluid availability in the different stages of zircon growth in order to provide reasonable interpretation for zircon U–Pb ages. In this paper, we presents a combined study of internal structure, U–Pb age and Lu–Hf isotopes for zircon, and O isotopes for mineral separates from UHP eclogites enclosed in marble from the Dabie orogen. The results not only provide insight into fluid regime in the bulk processes of continental subduction and exhumation, but also place geochronological constraints on timescale of UHP metamorphism.

2. Geological settings and samples

The Dabie-Sulu UHP metamorphic belt is a continental collision orogen between the South China Block and the North China Block (Cong, 1996; Liou et al., 1996; Zheng et al., 2003, 2005b). It is separated into eastern and western sections by the Tanlu Fault, which are named as the Sulu and Dabie orogens, respectively (Fig. 1). A series of continuous zones in the Dabie orogen were separated by several large-scale EW-trending faults, resulting in five main tectonic zones from north to south (Hacker et al., 2000; Zheng et al., 2005b): (1) the Beihuaiyang greenschist-facies zone, (2) the North Dabie high-T/UHP granulite-facies zone, (3) the Central Dabie medium-T/UHP eclogite-facies zone, (4) the South Dabie low-T/UHP eclogite-facies zone, and (5) the Susong blueschist-facies zone. All the five zones contain Early Cretaceous igneous intrusives (Jahn et al., 2003), with minor occurrence of coeval volcanic rocks in the northern two zones (Fan et al., 2004). Anatexis of orogenic lithospheric keel formed by the Triassic continent–continent collision is proposed for origin and genesis of these post-collisional igneous rocks (Zhao et al., 2004, 2005).

According to field occurrence and country-rock association (e.g., Wang et al., 1995; Cong, 1996; Zheng et al., 2003), three types of eclogite are recognized in the Dabie-Sulu orogenic belt: (1) G-type, gneiss-hosted enclaves or layers; (2) M-type, interlayers with or enclaves within marble or calc-silicate rocks; (3) P-type, either members of layered mafic-ultramafic intrusions or simply in association with ultramafic rocks (peridotite or pyroxenite). Previous studies of zircon U–Pb dating have been mostly devoted to the G-type eclogite (e.g., Ames et al., 1996; Rowley et al., 1997; Hacker et al., 1998, 2000; Ayers et al., 2002; Liu et al., 2004a,b, 2005; Zheng et al., 2004, 2005a), with a few to the P-type eclogite (Ayers et al., 2002; Rumble et al., 2002; Yang et al., 2003; Zhang et al., 2005). Thus this study examines the M-type eclogite in the Dabie orogen (Fig. 1).

Marbles in the Dabie orogen occur as lenses and bands in gneisses, containing eclogite boudins as blocks or bands.

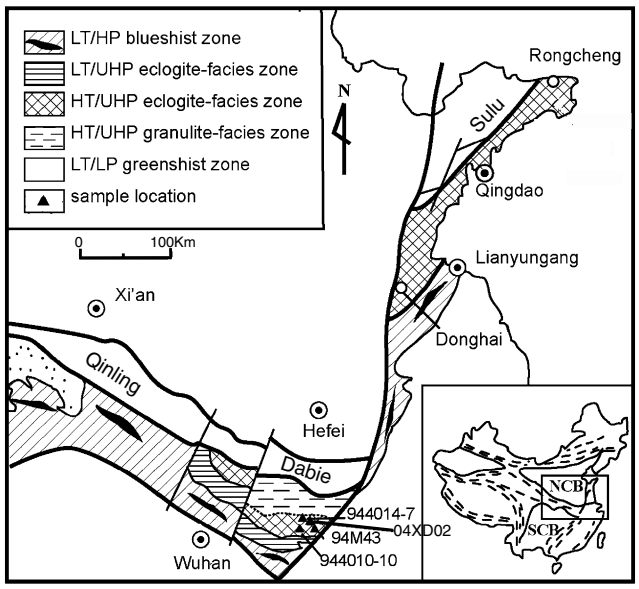

Fig. 1. Sketch map of geology in the Dabie-Sulu orogenic belt (revised after Wang et al., 1995), with sample locations of eclogite in association with ultrahigh-pressure marble in the Dabie orogen.

Coesite, partially inverted to quartz, occurs as inclusions within dolomite in the marbles (Schertl and Okay, 1994; Zhang and Liou, 1996). Coesite (Zhang and Liou, 1996) and diamond (Xu et al., 1992) inclusions were also found in the eclogite boudins within the marbles as well as in other eclogites in association with gneisses and pyroxenites (Xu et al., 2003, 2005). These indicate that the marbles and associated eclogites share the same UHP metamorphic history as the other eclogites. On the basis of the presence of diamond and coesite inclusions, peak metamorphic pressures were estimated to be greater than 3.3 GPa at temperatures of 700 to 800 °C based on garnet–clinopyroxene geothermometry (Cong, 1996; Okay, 1993; Carswell et al., 1997). The presence of unusually positive $\delta^{13}C$ values in the marbles indicates that their protolith was Neoproterozoic limestones on the Yangtze platform (Zheng et al., 1998a, 2003; Rumble et al., 2000).

Four samples of eclogite (944010-10, 944014-7, 94M43 and 04XD02) were selected for isotopic analyses in this study, which are all enclosed within the UHP marbles in the eastern part of the Central Dabie zone. They are located at Wangjiachong in Laoyoufang of the Shima area, Wangdawu in the Hengchong area, Shuanghe in the Pailou area, and Xindian in the Wumiao area, respectively (Fig. 1). They all occur as blocks within the marbles, with clear boundaries between the eclogites and the marbles. The eclogites contain garnet + omphacite ± phengite ± rutile ± zoisite/epidote ± quartz, with some accessory minerals such as apatite, zircon and titanite. Garnet and omphacite are partly replaced by amphibolite-facies symplectite composed of amphibole + plagioclase; rutile is partly transformed into titanite.

3. Analytical methods

Mineral separates were extracted by crushing, sieving and using heavy liquids, and then purified by hand picking under a binocular microscope. Transparent zircon grains without cracks were selected for U–Pb and Lu–Hf isotopic analyses. The zircons were mounted together with TEMORA standard in epoxy resin and then polished down to expose grain centres. CL images were collected using a JEOL JXA-8900RL electron microprobe at the Institute of Mineral Resources in the Chinese Academy of Geological Sciences, Beijing

Zircon U–Pb dating for three of the four samples was carried out using SHRIMP II at Beijing SHRIMP Center. Instrumental conditions and data acquisition methods follow Williams (1998). U and Th abundances were calibrated against standard zircon SL13. Zircon TEMORA (417 Ma) was used as a work standard (Black et al., 2003), which was analyzed every fourth analysis. The measured ^{204}Pb was used for common Pb correction. The data were reduced using the ISOPLOT program (Ludwig, 2001). Individual analyses were reported with 2σ uncertainties; weighted average of ages was also reported at the 2σ level.

Zircon U–Pb dating for the fourth sample (04XD02) was made by means of LA-ICPMS at Northwest University in Xi'an. The detailed analytical procedure is described in Yuan et al. (2004). The GeoLas 200M laser-ablation system equipped with a 193 nm ArF-excimer laser was used in connection with an ELAN6100 DRC ICP-MS. Helium was used as the carrier gas to enhance the transport efficiency of the ablated material. The helium carrier gas inside the ablation cell is mixed with argon as a makeup gas before entering the ICP to maintain stable and optimum excitation conditions. The spot diameter was 30 μm. Each analysis includes a background acquisition interval of approximately 30 s and a signal acquisition of about 80 s. Raw data were processed using the Glitter program. All measurements were normalized relative to zircon 91500, with a recommended $^{206}Pb/^{238}U$ age of 1065.4 ± 0.6 Ma (Wiedenbeck et al., 1995). Standard silicate glass NIST SRM610 was used to calculate U, Th and Pb concentrations. The common Pb correction was carried out by using the EXCEL program of ComPbCorr#_151 (Andersen, 2002), assuming $t = 230$ Ma for time of both Pb loss and common Pb growth.

Zircon Lu–Hf isotope analysis was carried out by means of LA-MC-ICPMS at the Institute of Geology and Geophysics, the Chinese Academy of Sciences, Beijing. Instrumental conditions were described by Xu et al. (2004). A Geolas-193 laser-ablation microprobe was attached to a Neptune multi-collector ICPMS. The analyses were conducted with a beam diameter of 32 μm with a typical ablation time of about 30 s for 200 cycles of each measurement, a 10 Hz repetition rate, and a laser power of 100 mJ/pulse (Wu et al., 2006). Both He and Ar carrier gas transported the ablated sample from the laser-ablation cell via a mixing chamber to the ICPMS torch. Isobaric interference of ^{176}Lu on ^{176}Hf was corrected by measuring the intensity of the interference-free ^{175}Lu isotope and using a recommended $^{176}Lu/^{175}Lu$ ratio of 0.02669 (DeBievre and Taylor, 1993) to calculate $^{176}Lu/^{177}Hf$. Similarly, isobaric interference of ^{176}Yb on ^{176}Hf was corrected by measuring the interference-free ^{172}Yb isotope and using a recommended $^{176}Yb/^{172}Yb$ ratio of 0.5886 (Chu et al., 2002) to calculate $^{176}Hf/^{177}Hf$ ratios. In doing so, a mean $^{173}Yb/^{171}Yb$ ratio for the analysed spot itself was automatically used in the same run to calculate a mean β_{Yb} value, and then the ^{176}Yb signal intensity was calculated from the ^{173}Yb signal intensity and the mean β_{Yb} value (Iizuka and Hirata, 2005). Following the suggestion of Woodhead et al. (2004), five standard zircons (91500, TEMORA, CZ3, CN92-1 and FM0411) were used in this correction to the ^{176}Yb–^{176}Hf interference. They show variable $^{176}Yb/^{177}Hf$ ratios of 0.0066–0.0126 with an average 0.0077 for 91500, 0.018–0.038 with an average 0.032 for TEMORA, 0.00091–0.00125 with an average 0.00099 for CZ3, 0.0106–0.0320 with an average 0.020 for CN92-1, and 0.0045–0.0068 with an average 0.0058 for FM0411 (Wu et al., 2006). TEMORA has the highest Yb/Hf ratios and thus more precise β_{Yb} factor and $^{176}Hf/^{177}Hf$ ratios than the others. Therefore,

TEMORA is an appropriate reference for the isobaric interference correction. On the other hand, CZ3 has the lowest $^{176}Yb/^{177}Hf$ ratios, so that only about 10 and 20 ppm maximum deviation were caused by the Yb interference correction for $^{176}Hf/^{177}Hf$ ratios when using 63 or 32 μm spot size.

Zircon 91500 was used as the reference standard, with a recommended $^{176}Hf/^{177}Hf$ ratio of 0.282293 ± 28 (Woodhead et al., 2004), and our analyses gave $^{176}Hf/^{177}Hf$ ratios of 0.282307 ± 31 for it (Wu et al., 2006). All the Lu–Hf isotope analysis results are reported with the error in 2σ of the mean, and statistical treatment proceeds by means of the ISOPLOT program of Ludwig (2001). We have adopted a decay constant for ^{176}Lu of $1.865 \times 10^{-11}\ yr^{-1}$ (Scherer et al., 2001). Initial $^{176}Hf/^{177}Hf$ ratio, denoted as $\varepsilon_{Hf}(t)$, is calculated relative to the chondritic reservoir with a $^{176}Hf/^{177}Hf$ ratio of 0.282772 and $^{176}Lu/^{177}Hf$ of 0.0332 (Blichert-Toft and Albarede, 1997). Single-stage Hf model ages (T_{DM1}) are calculated relative to the depleted mantle with a present-day $^{176}Hf/^{177}Hf$ ratio of 0.28325 and $^{176}Lu/^{177}Hf$ of 0.0384 (Vervoort and Blichert-Toft, 1999).

Oxygen isotope analysis of mineral separates was conducted by the laser fluorination technique using a 25 W MIR-10 CO_2 laser at University of Science and Technology of China in Hefei. About 1.5 to 2.0 mg mineral grains were reacted with BF_5 to release O_2, which was directly transferred to a Finnigan Delta+ mass spectrometer for measurement of $^{18}O/^{16}O$ and $^{17}O/^{16}O$ ratios (Zheng et al., 2002). Oxygen isotope data are reported in the $\delta^{18}O$ notation with the reference to VSMOW standard. Three reference minerals were used: $\delta^{18}O = 5.8 \pm 0.1‰$ for UWG-2 garnet (Valley et al., 1995), $\delta^{18}O = 11.11 \pm 0.1‰$ for GBW04409 quartz (Zheng et al., 1998b), and $\delta^{18}O = 10.0 \pm 0.1‰$ for 91500 zircon (Zheng et al., 2004).

4. Results

4.1. Zircon morphology

Typical CL pictures are presented in Fig. 2. Zircons in sample 944010-10 are anhedral to subhedral. Most of them are oval, and a few crystals are short prismatic or irregular with multi-faceted characteristics. Lengths of these grains range from 50 to 200 μm, with aspect ratios of 1:1 to 2:1. Most of them have weak CL brightness core and relatively strong CL brightness rim, showing no zoning to weakly zoning. A few crystals have planar zoning (Fig. 2a). All the zonations are typical for metamorphic growth (Vavra et al., 1999; Hoskin and Black, 2000; Wu and Zheng, 2004; Zheng et al., 2004). Resorption structures are preserved around the cores of some grains (Fig. 2a). A few grains are found to have pitted surface and cloudy zoning, suggesting different conditions of formation.

Zircons from sample 944014-7 are colorless, translucent, anhedral to subhedral. The lengths of these crystals range from 50 to 100 μm, with ratios of length to width ranging from 1:1 to 2.5:1. They are oval to round in shape. A few of them are short prismatic. In CL images (Fig. 2b), most of them reveal sector zoning or fir-tree zoning, while some grains just show weak zoning or cloudy zoning. They are interpreted as metamorphic growth. Homogenous rims with relatively strong CL brightness occur around these zircons, suggesting that they were disturbed by late metamorphic event after their formation. A few grains have irregular shape and clear pitted surface. The CL imaging reveals that they are homogeneous with relatively strong CL brightness, and some domains show patchy zoning.

Zircon grains in sample 94M43 have oval or short prismatic shape. Their lengths range from 50 to 150 μm, with aspect ratios of 1:1 to 2:1. In CL images (Fig. 2c), most zircons have distinct core-rim structure. The cores have irregular shape, showing no zoning with relatively strong or weak brightness in CL images, which may be inherited detrital zircons that suffered different degrees of metamorphic recrystallization (Hoskin and Black, 2000; Tomaschek et al., 2003). The rims show weak zoning or cloudy zoning in CL images, which may represent metamorphic overgrowth (Rowley et al., 1997; Hacker et al., 1998; Ayers et al., 2002).

Zircons in sample 04XD02 are transparent, colorless and anhedral. They range in length from 100 to 200 μm, and have length to width ratios of about 1:1 to 3:1. Based on CL images, three domains, which are core, mantle and rim, can be discerned. The cores have variable internal zoning pattern and only present in a few grains, which may represent inherited zircons that were differently modified by metamorphic recrystallization (Hoskin and Black, 2000; Tomaschek et al., 2003). The mantles are unzoned or weakly zoned, and are commonly embayed by the rims. They have different CL brightness, even within a single mantle domain (Fig. 2d), indicating that they may grow under unstable conditions. Discontinuously homogeneous rims occur around most grains, which may form by a late metamorphic event.

4.2. Zircon U–Pb ages

Eight U–Pb analyses were obtained from 8 zircon grains in eclogite 944010-10 from Laoyoufang (Table 1). Except for analysis 4.1 that has a relatively low U content of 102 ppm and a high Th/U ratio of 0.485, the other seven analyses yield U concentrations of 206–1807 ppm and Th of 6.0–48.1 ppm, with Th/U ratios of 0.016–0.044. They are all concordant in U–Pb ages within 1σ uncertainty (Fig. 3a), and have very similar $^{206}Pb/^{238}U$ ages of 245 ± 4 to 237 ± 4 Ma (Table 1). All the eight analyses yield a weighted mean $^{206}Pb/^{238}U$ age of 242 ± 3 Ma (MSWD = 0.38).

Eight zircon grains from eclogite 944014-7 at Hengchong were dated by eight analyses (Table 1). The eight analyses show low U abundances of 59–94 ppm and very low Th abundances of 0.63–1.38 ppm, resulting in very low Th/U ratios of 0.008–0.014. The proportion of com-

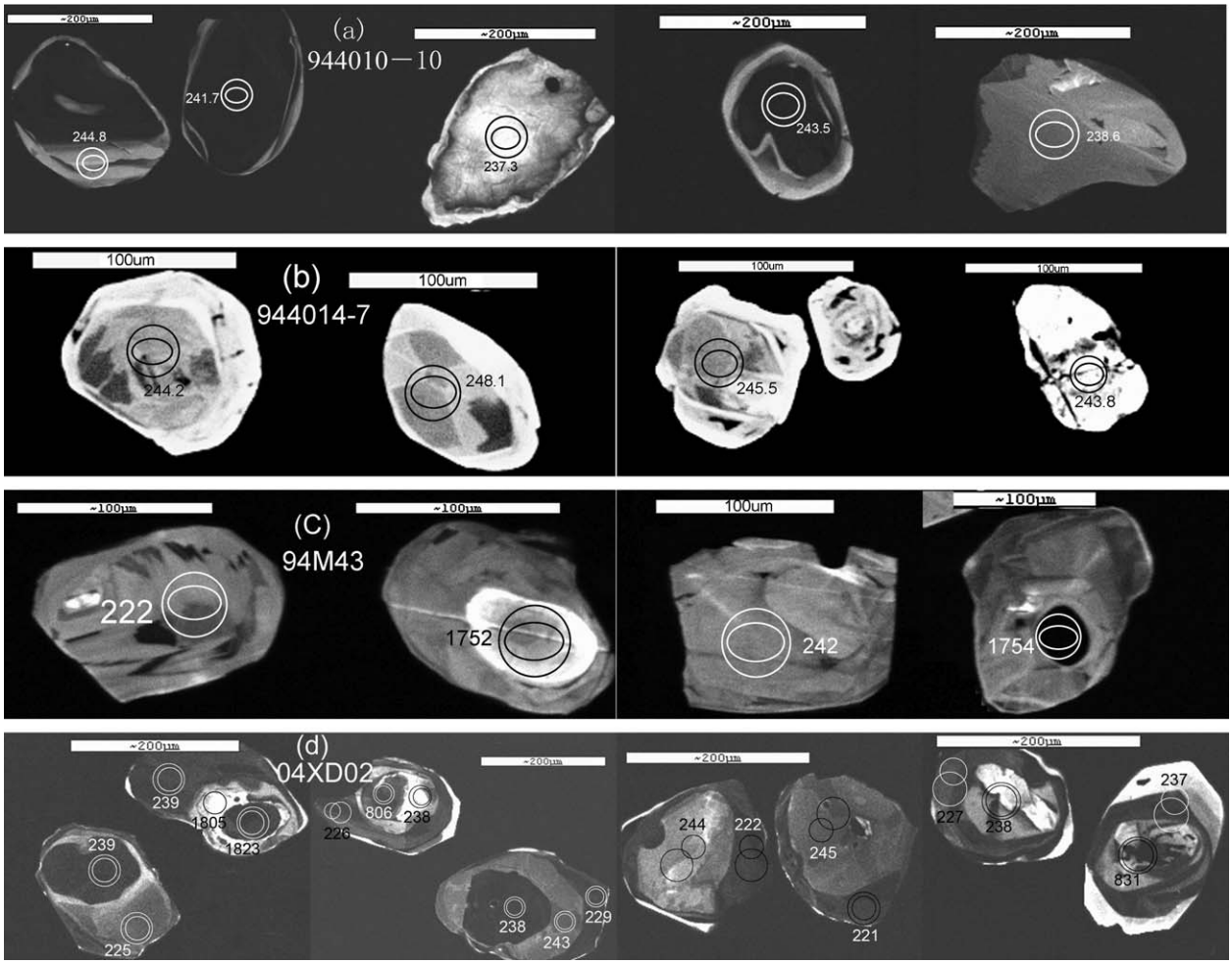

Fig. 2. Typical CL images of zircons with $^{206}Pb/^{238}U$ ages for eclogite enclosed in marble in the Dabie orogen. Small circles show the sites of U–Pb dating, and big circles denote the locations of Lu–Hf isotope analysis. (a) Shima, (b) Hengchong, (c) Shuanghe, and (d) Xindian.

mon Pb is relatively high (3.00–9.23%). These chemical features are common for metamorphic zircon (Tomaschek et al., 2003). All the eight analyses are concordant with consistent $^{206}Pb/^{238}U$ ages of 248 ± 5 to 243 ± 4 Ma (Fig. 3b), yielding a weighted mean of 245 ± 3 Ma (MSWD = 0.20). No precise age can be obtained from the homogeneous rim of high CL brightness because it is too thin to be analyzed by SHRIMP (Fig. 2b).

Thirteen SHRIMP U–Pb analyses were made on twelve zircon grains from eclogite 94M43 at Shuanghe (Table 1). Analyses of five inherited core yield moderate U and Th contents with Th/U ratios of 0.042 to 0.260, and $^{206}Pb/^{238}U$ ages of 292 ± 4 to 1311 ± 17 Ma; whereas the remaining eight analyses on metamorphic zircon show relatively low Th contents of 3.4–6.5 ppm and Th/U ratios of 0.019–0.027, and $^{206}Pb/^{238}U$ ages of 222 ± 4 to 246 ± 4 Ma (Table 1 and Fig. 3c). In the U–Pb concordia diagram (Fig. 3c), all the 13 analyses define a discordia with intercept ages of 1816 ± 14 Ma and 234 ± 7 Ma, respectively. The young ages are further subdivided into two groups with one at 242 ± 4 Ma ($n = 4$, MSWD = 0.60) and the other at 226 ± 4 Ma ($n = 4$, MSWD = 0.54), respectively.

A total of 30 U–Pb analyses were carried out by LA-ICPMS on 13 zircon grains from eclogite 04XD02 at Xindian (Table 2 and Fig. 3d). Six analyses on four inherited cores have variable U and Th concentrations, and their apparent $^{206}Pb/^{238}U$ ages scatter between 790 and 1422 Ma. Four of them are nearly concordant, and give a weighted average $^{206}Pb/^{238}U$ age of 812 ± 30 Ma (MSWD = 1.7). The other two analyses are discordant, and yield indistinguishable $^{207}Pb/^{206}Pb$ ages of 1805 ± 17 and 1823 ± 65 Ma (mean = 1806 ± 32 Ma). Therefore, there are two generations of inherited zircon in this sample. Thirteen analyses on the mantle domains have moderate U contents of 125–610 ppm and Th of 2.3–15.9 ppm, with very low Th/U ratios of 0.01–0.03. All the spots are concordant or nearly concordant (Fig. 3d). $^{206}Pb/^{238}U$ age varies from 237 ± 3 to 245 ± 3 Ma, with a weighted mean of 240 ± 2 Ma (MSWD = 0.78). The other 11 analyses of the rim domains have similar U and Th contents of 121–619 ppm and 1.3–41.8 ppm, respectively, and also very low Th/U ratios of 0.01–0.07. All the eleven analyses yield $^{206}Pb/^{238}U$ ages of 216 ± 3 to 229 ± 3 Ma with a weighted mean of 223 ± 2 Ma (MSWD = 1.4) (Fig. 3d).

Table 1
SHRIMP zircon U–Pb isotope data for eclogites enclosed in the marbles in the Dabie orogen

Spot	$^{206}Pb_c$ (%)	U (ppm)	Th (ppm)	Th/U	$^{206}Pb^*$ (ppm)	$^{207}Pb^*/^{206}Pb^*$	±%	$^{207}Pb^*/^{235}U$	±%	$^{206}Pb^*/^{238}U$	±%	err corr	$^{206}Pb/^{238}U$ Age	±2σ	$^{207}Pb/^{206}Pb$ Age	±2σ
944010-10 (Laoyoufang)																
1.1	0.21	1807	28.2	0.016	62.1	0.05061	1.8	0.2666	2.5	0.0382	1.6	0.924	241.7	3.9	223	42
2.1	1.33	255	6.0	0.024	8.59	0.05084	2.9	0.2713	3.7	0.0387	1.7	0.347	244.8	4.2	234	67
3.1	1.28	206	8.7	0.044	6.93	0.05077	2.8	0.2702	3.6	0.0386	1.7	0.388	244.1	4.2	230	65
4.1	1.19	102	48.1	0.485	3.34	0.05087	3.1	0.2630	4.1	0.0375	1.8	0.283	237.3	4.3	235	72
5.1	0.86	1546	32.4	0.021	46.8	0.05068	1.7	0.2690	2.6	0.0385	1.6	0.758	243.5	4.0	226	39
6.1	0.53	1237	36.3	0.029	35.1	0.05072	2.6	0.2685	3.5	0.0384	1.8	0.614	242.9	4.5	228	60
7.1	1.12	894	16.8	0.019	26.4	0.05081	2.8	0.2669	3.2	0.0381	1.7	0.419	241.0	4.2	232	65
8.1	0.34	358	12.7	0.035	15.6	0.05073	3.1	0.2637	3.9	0.0377	1.9	0.527	238.6	4.6	229	72
944014-7 (Hengchong)																
1.1	3.00	94	0.85	0.009	3.21	0.05085	2.6	0.2707	3.3	0.03861	1.8	0.114	244.2	4.5	234	60
2.1	3.40	80	1.04	0.013	2.85	0.05096	2.2	0.2728	2.6	0.03882	1.7	0.144	245.5	4.2	239	51
3.1	3.79	84	0.63	0.008	2.94	0.05173	2.9	0.2798	3.7	0.03923	1.8	0.101	248.1	4.5	273	67
4.1	9.23	59	0.80	0.014	2.46	0.05049	3.1	0.2676	3.6	0.03844	2.1	0.117	243.2	5.2	218	72
5.1	4.67	78	1.38	0.018	1.98	0.05124	3.1	0.2736	3.5	0.03872	1.9	0.214	244.9	4.7	252	70
6.1	7.21	64	1.26	0.020	2.56	0.05218	2.6	0.2814	2.9	0.03911	1.6	0.178	247.3	3.9	293	58
7.1	6.48	81	1.19	0.015	3.08	0.05087	2.4	0.2703	3.1	0.03854	1.8	0.193	243.8	4.5	235	54
8.1	3.38	75	0.74	0.010	2.62	0.05106	2.8	0.2701	3.4	0.03836	1.7	0.162	242.7	4.1	244	65
Spot	$^{206}Pb_c$ (%)	U (ppm)	Th (ppm)	Th/U	$^{206}Pb^*$ (ppm)	$^{207}Pb^*/^{206}Pb^*$	±%	$^{207}Pb^*/^{235}U$	±%	$^{206}Pb^*/^{238}U$	±%	err corr	$^{206}Pb/^{238}U$ Age	±	$^{207}Pb/^{206}Pb$ Age	±
94M43 (Shuanghe)																
1.1	1.81	145	3.6	0.026	4.59	0.0504	4.2	0.2518	5.1	0.0362	1.8	0.239	229	4	216	97
1.2	1.62	163	3.4	0.021	5.03	0.0505	3.9	0.2493	4.7	0.0358	1.5	0.413	227	4	218	68
2.1	0.18	180	3.5	0.020	6.08	0.0575	2.2	0.3086	2.7	0.0389	1.7	0.600	246	4	511	48
3.1	3.08	300	75.5	0.260	16.4	0.0861	3.6	0.9699	4.7	0.0817	1.9	0.484	506	10	1340	70
4.1	0.52	112	24.5	0.225	20.1	0.1072	1.5	3.0596	1.9	0.2070	1.7	0.853	1213	23	1752	27
5.1	0.57	258	6.3	0.025	7.81	0.0505	1.4	0.2444	2.8	0.0351	1.6	0.418	222	4	218	32
6.1	2.15	169	3.9	0.024	5.63	0.0508	3.5	0.2664	4.1	0.0380	1.8	0.226	240	4	234	81
7.1	8.99	246	38.4	0.161	13.9	0.0767	2.9	0.6335	3.8	0.0599	1.9	0.207	375	7	1113	58
8.1	0.02	209	8.5	0.042	40.4	0.1073	1.8	3.3362	2.5	0.2255	1.2	0.951	1311	17	1754	33
9.1	4.85	201	18.1	0.093	8.39	0.0625	3.7	0.3987	5.2	0.0463	1.4	0.169	292	4	690	79
10.1	1.26	227	4.2	0.019	6.57	0.0509	3.1	0.2498	3.8	0.0356	1.7	0.357	226	4	236	72
11.1	0.98	186	5.1	0.027	4.92	0.0511	2.2	0.2691	2.9	0.0382	1.3	0.568	242	3	245	51
12.1	1.67	169	3.9	0.023	7.16	0.0507	2.4	0.2642	3.1	0.0378	1.5	0.413	239	4	227	55

Notes. Pb_c and Pb^* denote the common and radiogenic portions, respectively; errors are reported in 2σ.

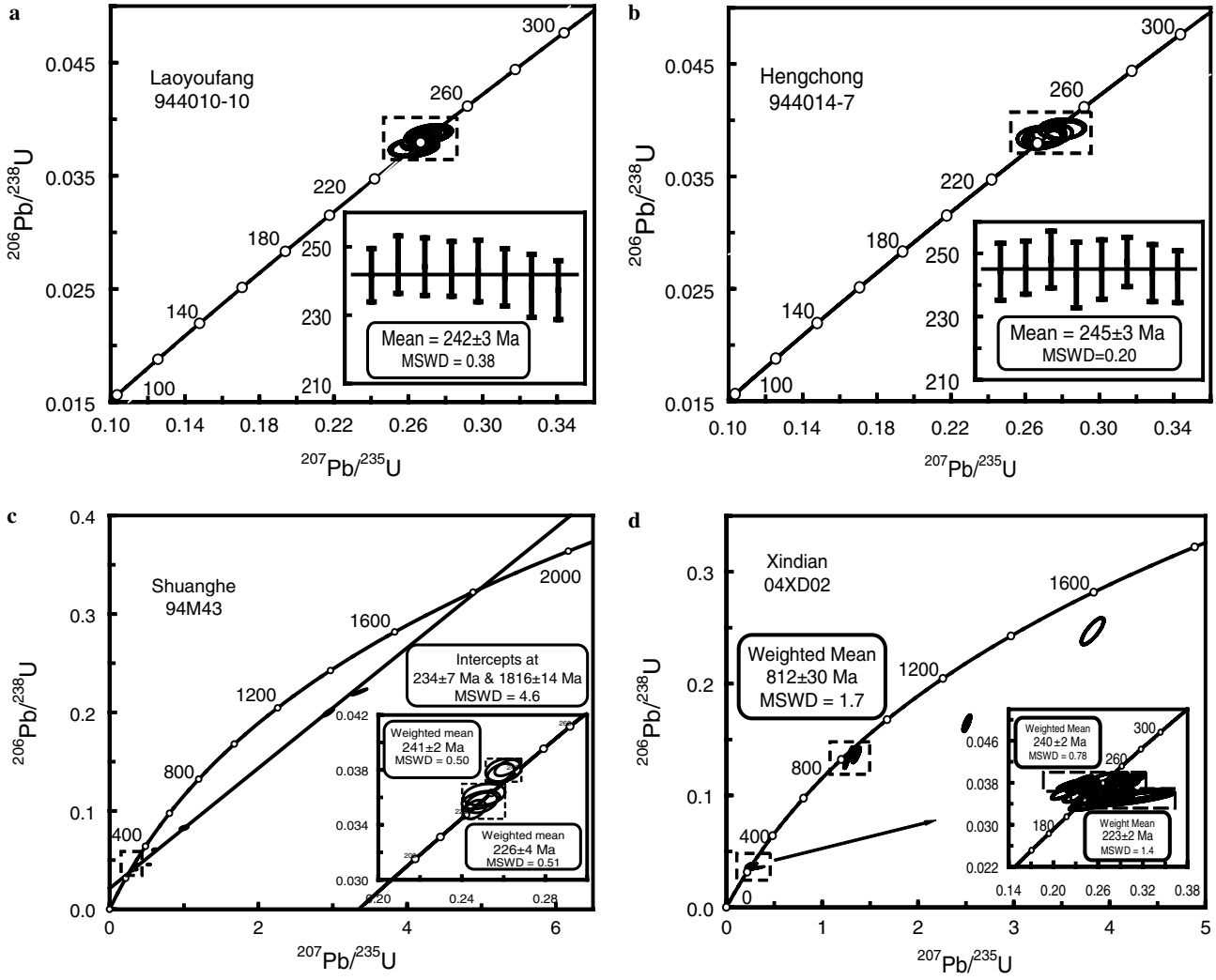

Fig. 3. Concordia diagrams of zircon U–Pb isotope data for eclogite enclosed in marble in the Dabie orogen. (a) Shima, (b) Hengchong, (c) Shuanghe, and (d) Xindian.

4.3. Zircon Lu–Hf isotopes

Fifteen analyses for Lu–Hf isotope composition were made on 15 zircon grains from eclogite 944010-10 at Laoyoufang, including 9 spots that were dated by the SHRIMP U–Pb technique to give consistent Triassic ages (Table 3). Except for analysis #1 that has a relatively high $^{176}Lu/^{177}Hf$ ratio of 0.000383, all other analyses exhibit very low $^{176}Lu/^{177}Hf$ ratios of 0.000005–0.000009. Nevertheless, all of the 15 analyses yield similar $^{176}Hf/^{177}Hf$ ratios of 0.281986–0.282089. If the metamorphic age of 242 Ma is used, they yield $\varepsilon_{Hf}(t)$ values of -22.5 to -18.9 with a weighted mean of -20.6 ± 1.4 (MSWD = 7.1).

Ten Lu–Hf analyses were obtained for 10 grains of metamorphic zircon in eclogite 944014-7 at Hengchong (Table 3), among which 8 spots have been dated with the U–Pb method to yield consistent Triassic ages. Except for analyses #4, #5 and #6 that have high $^{176}Lu/^{177}Hf$ ratios of 0.000192–0.000259, the others seven analyses show very low $^{176}Lu/^{177}Hf$ ratios of 0.000001–0.000006. Nevertheless, all of the 10 analyses have similar $^{176}Hf/^{177}Hf$ ratios in the range of 0.282120–0.282163, corresponding to $\varepsilon_{Hf}(t)$ values of -17.7 to -16.2, with a weighted mean of -16.9 ± 0.7 (MSWD = 1.08) at $t = 245$ Ma.

Fifteen analyses for Lu–Hf isotope composition were made for 15 zircons in eclogite 94M43 at Shuanghe, including 11 analyses of the grains that have been dated with the U–Pb method (Table 3). Six analyses (#1, #7 to #10 and #13) were obtained from the inherited domains of core as identified by their greater $^{206}Pb/^{238}U$ ages than 245 Ma, which show high $^{176}Lu/^{177}Hf$ ratios of 0.000115–0.000286 but low $^{176}Hf/^{177}Hf$ ratios of 0.282049–0.282223. The other nine analyses were obtained from the Triassic domains of metamorphic overgrowth with low $^{176}Lu/^{177}Hf$ ratios of 0.000004–0.000007 but high $^{176}Hf/^{177}Hf$ ratios of 0.282245 to 0.282345. $\varepsilon_{Hf}(t)$ values are calculated by assuming $t = 240$ Ma, yielding a range from -20.4 to -14.1 with a weighted mean of -16.7 ± 2.7 (MSWD = 29) for the inherited cores (Fig. 4c), which are lower than those

Table 2
LA-ICPMS zircon U–Pb dating for eclogite 04XD02 at Xindian in the Dabie orogen

Spot	U (ppm)	Th (ppm)	Th/U	$^{206}Pb^{*}$ (ppm)	$^{207}Pb^{*}/^{206}Pb^{*}$	±	$^{207}Pb^{*}/^{235}U$	±	$^{206}Pb^{*}/^{238}U$	±	$^{206}Pb/^{238}U$ Age	±	$^{207}Pb/^{235}U$ Age	±	$^{207}Pb/^{206}Pb$ Age	±
1.1	610	3.4	0.01	25.78	0.04419	0.00049	0.22543	0.00793	0.03761	0.00040	238	3	206	8	−100	27
1.2	164	3.3	0.02	8.47	0.05320	0.00138	0.28307	0.00680	0.03834	0.00063	243	4	253	7	338	59
1.3	411	11.4	0.03	16.54	0.04519	0.00057	0.21571	0.00718	0.03619	0.00052	229	3	198	7	−45	31
2.1	388	9.2	0.02	16.65	0.04877	0.00065	0.24071	0.00549	0.03785	0.00047	239	3	219	6	137	31
2.2	318	13.9	0.04	15.01	0.05506	0.00092	0.29034	0.00707	0.03500	0.00042	222	3	259	7	415	37
3.1	368	7.2	0.02	58.20	0.06927	0.00135	1.28058	0.01986	0.13322	0.00218	806	14	837	20	907	40
3.2	160	4.0	0.02	7.46	0.04907	0.00084	0.24305	0.00378	0.03769	0.00066	238	4	221	4	151	40
3.3	451	14.1	0.03	16.27	0.04939	0.00155	0.23819	0.00994	0.03575	0.00056	226	4	217	10	167	73
4.1	452	3.4	0.01	19.70	0.04484	0.00065	0.23467	0.00681	0.03771	0.00061	239	4	214	7	−64	35
4.2	261	8.5	0.03	13.06	0.05850	0.00077	0.28803	0.00899	0.03548	0.00045	225	3	257	9	549	29
5.1	1626	74.9	0.05	393.88	0.07171	0.00099	1.35514	0.01576	0.13618	0.00261	823	17	870	16	978	28
5.2	615	24.4	0.04	102.64	0.06927	0.00067	1.25199	0.00846	0.13029	0.00226	790	15	824	9	907	20
5.3	530	4.7	0.01	28.83	0.05485	0.00181	0.26352	0.00826	0.03482	0.00042	221	3	237	8	406	74
6.1	408	26.3	0.06	135.73	0.11146	0.00398	3.82193	0.04746	0.24687	0.00483	1422	31	1597	47	1823	65
6.2	99	2.5	0.03	17.31	0.11032	0.00106	2.50915	0.01555	0.16443	0.00281	981	18	1275	16	1805	17
6.3	358	15.9	0.04	15.67	0.04822	0.00066	0.23922	0.00856	0.03771	0.00035	239	2	218	9	110	32
7.1	125	3.8	0.03	5.54	0.05405	0.00101	0.28249	0.00470	0.03766	0.00041	238	3	253	5	373	42
7.2	319	9.6	0.03	15.12	0.05525	0.00088	0.27081	0.00358	0.03532	0.00038	224	2	243	4	422	36
8.1	277	2.9	0.01	13.56	0.04897	0.00069	0.26313	0.00732	0.03872	0.00044	245	3	237	7	146	33
8.2	378	13.4	0.04	15.71	0.05014	0.00073	0.24039	0.00612	0.03485	0.00057	221	4	219	6	201	34
9.1	236	7.4	0.03	9.60	0.05593	0.00174	0.29897	0.00934	0.03852	0.00038	244	2	266	9	450	69
9.2	619	41.3	0.07	22.89	0.06289	0.00507	0.30528	0.02313	0.03498	0.00056	222	4	271	23	705	172
10.1	1352	56.1	0.04	295.80	0.06799	0.00078	1.29865	0.01084	0.13765	0.00214	831	14	845	11	868	24
10.2	370	10.6	0.03	19.35	0.05621	0.00122	0.29155	0.00909	0.03738	0.00045	237	3	260	9	460	48
11.1	172	2.3	0.01	7.38	0.05176	0.00097	0.27027	0.00872	0.03763	0.00037	238	2	243	9	275	43
11.2	417	8.4	0.02	16.99	0.05149	0.00124	0.25603	0.00674	0.03583	0.00039	227	3	231	7	263	55
12.1	239	6.1	0.03	10.35	0.05166	0.00127	0.27136	0.00812	0.03785	0.00040	239	3	244	8	271	56
12.2	467	13.8	0.03	16.71	0.05549	0.00296	0.25421	0.01327	0.03401	0.00050	216	3	230	13	432	119
13.1	255	5.9	0.02	10.84	0.05431	0.00108	0.28723	0.01052	0.03811	0.00051	241	3	256	11	384	45
13.2	121	1.3	0.01	4.51	0.06195	0.01109	0.30518	0.02121	0.03556	0.00049	225	3	270	21	672	383

Notes. Pb^{*} denotes the radiogenic lead; errors are reported in 2σ.

Table 3
Zircon Lu–Hf isotope compositions for eclogites in marble in the Dabie-Sulu orogen

No.	$^{176}Yb/^{177}Hf$	$^{176}Lu/^{177}Hf$	$^{176}Hf/^{177}Hf$	±	$t_{6/8}$ (Ma)*	$\varepsilon_{Hf}(0)$	$\varepsilon_{Hf}(t)$*	±	T_{DM1} (Ma)	±
944010-10 (Laoyoufang)										
1	0.010115	0.000383	0.282054	0.000014	237.3	−25.4	−20.1	0.5	1661	39
2	0.000277	0.000009	0.282028	0.000010	241.1	−26.3	−21.0	0.4	1681	28
3	0.000227	0.000007	0.282074	0.000013	244.8	−24.7	−19.4	0.5	1618	36
4	0.000200	0.000006	0.282068	0.000011	244.1	−24.9	−19.6	0.4	1626	31
5	0.000182	0.000005	0.282089	0.000012	243.5	−24.2	−18.9	0.4	1598	33
6	0.000212	0.000006	0.282005	0.000014	242.9	−27.1	−21.8	0.5	1711	38
7	0.000222	0.000007	0.282062	0.000012	241.0	−25.1	−19.8	0.4	1633	34
8	0.000204	0.000006	0.281992	0.000012	238.6	−27.6	−22.3	0.4	1729	33
9	0.000268	0.000009	0.282040	0.000013		−25.9	−20.6	0.5	1664	35
10	0.000157	0.000005	0.281986	0.000013		−27.8	−22.5	0.5	1736	36
11	0.000219	0.000006	0.282088	0.000012		−24.2	−18.9	0.4	1598	33
12	0.000238	0.000007	0.282037	0.000014		−26.0	−20.7	0.5	1668	39
13	0.000243	0.000007	0.282005	0.000016		−27.1	−21.8	0.6	1711	43
14	0.000168	0.000005	0.282012	0.000015		−26.9	−21.6	0.5	1701	40
15	0.000192	0.000006	0.282019	0.000014		−26.6	−21.3	0.5	1692	38
944014-7 (Hengchong)										
1	0.000055	0.000002	0.282120	0.000015	244.2	−23.1	−17.7	0.5	1555	40
2	0.000077	0.000005	0.282137	0.000014	245.5	−22.4	−17.1	0.5	1532	38
3	0.000052	0.000002	0.282156	0.000016	248.1	−21.8	−16.4	0.6	1506	44
4	0.003767	0.000233	0.282161	0.000013	244.9	−21.6	−16.3	0.5	1509	35
5	0.007805	0.000259	0.282129	0.000015	243.8	−22.7	−17.4	0.5	1553	41
6	0.005632	0.000192	0.282160	0.000017	247.3	−21.7	−16.3	0.6	1509	47
7	0.000050	0.000001	0.282140	0.000023		−22.4	−17.0	0.8	1529	63
8	0.000082	0.000006	0.282146	0.000020		−22.1	−16.8	0.7	1520	54
9	0.000079	0.000005	0.282125	0.000013		−22.9	−17.5	0.5	1548	36
10	0.000055	0.000002	0.282163	0.000019		−21.5	−16.2	0.7	1497	53
94M43 (Shuanghe)										
1	0.001646	0.000131	0.282130	0.000013	506.0	−22.7	−17.5	0.5	1547	35
2	0.000126	0.000004	0.282311	0.000013	229.0	−16.3	−11.1	0.5	1296	35
3	0.000108	0.000004	0.282345	0.000012	246.0	−15.1	−9.8	0.4	1249	33
4	0.000108	0.000004	0.282334	0.000011	226.0	−15.5	−10.2	0.4	1264	30
5	0.000121	0.000004	0.282338	0.000012	242.0	−15.3	−10.1	0.4	1259	33
6	0.000116	0.000004	0.282270	0.000011	240.0	−17.8	−12.5	0.4	1351	30
7	0.001511	0.000124	0.282219	0.000011	375.0	−19.6	−14.3	0.4	1425	30
8	0.003676	0.000286	0.282086	0.000013	1311.0	−24.3	−19.0	0.5	1613	35
9	0.001314	0.000115	0.282223	0.000013	292.0	−19.4	−14.1	0.5	1419	35
10	0.003003	0.000253	0.282049	0.000013	1213.0	−25.6	−20.4	0.5	1662	35
11	0.000152	0.000005	0.282286	0.000011	222.0	−17.2	−11.9	0.4	1330	30
12	0.000127	0.000004	0.282253	0.000011		−18.4	−13.1	0.4	1375	30
13	0.001622	0.000128	0.282172	0.000016		−21.2	−16.0	0.6	1489	43
14	0.000177	0.000007	0.282292	0.000017		−17.0	−11.7	0.6	1322	46
15	0.000094	0.000004	0.282245	0.000012		−18.6	−13.4	0.4	1385	33
04XD02 (Xindian)										
1	0.000165	0.000007	0.283161	0.000023	238	13.7	18.9	0.8	125	65
2	0.000072	0.000003	0.283132	0.000027	243	12.7	17.8	1.0	165	76
3	0.000100	0.000004	0.283048	0.000025	229	9.8	14.9	0.9	281	70
4	0.000120	0.000005	0.283137	0.000034	239	12.9	18.0	1.2	157	95
5	0.000085	0.000004	0.283126	0.000026	222	12.5	17.6	0.9	173	73
6	0.002806	0.000128	0.282907	0.000024	806	4.7	9.8	0.9	479	67
7	0.000145	0.000007	0.282834	0.000030	238	2.2	7.3	1.1	577	82
8	0.000090	0.000004	0.283058	0.000025	225	10.1	15.2	0.9	268	69
9	0.000059	0.000003	0.283083	0.000025	239	11.0	16.1	0.9	233	69
10	0.003107	0.000157	0.282733	0.000035	823	−1.4	3.7	1.2	720	96
11	0.000286	0.000013	0.282814	0.000030	239	1.5	6.6	1.1	606	82
12	0.005985	0.000341	0.282307	0.000031	1422	−16.5	−11.4	1.1	1313	86
13	0.000097	0.000004	0.283011	0.000028	239	8.5	13.6	1.0	333	77
14	0.000243	0.000012	0.283188	0.000042	238	14.7	19.8	1.5	86	116
15	0.000087	0.000005	0.283124	0.000031	224	12.4	17.6	1.1	176	87
16	0.000506	0.000028	0.283096	0.000028	245	11.4	16.6	1.0	215	78

(*continued on next page*)

Table 3 (*continued*)

No.	$^{176}Yb/^{177}Hf$	$^{176}Lu/^{177}Hf$	$^{176}Hf/^{177}Hf$	±	$t_{6/8}$ (Ma)*	$\varepsilon_{Hf}(0)$	$\varepsilon_{Hf}(t)$*	±	T_{DM1} (Ma)	±
17	0.000066	0.000003	0.283095	0.000026	221	11.4	16.6	0.9	215	72
18	0.000068	0.000003	0.283059	0.000024	222	10.2	15.3	0.8	266	66
19	0.000397	0.000017	0.282631	0.000029	244	−5.0	0.1	1.0	858	81
20	0.003089	0.000149	0.282846	0.000033	831	2.6	7.7	1.2	563	92
21	0.000159	0.000007	0.282692	0.000039	237	−2.8	2.3	1.4	774	107
22	0.000114	0.000006	0.283093	0.000029	238	11.4	16.5	1.0	219	81
23	0.000106	0.000005	0.282959	0.000039	227	6.6	11.7	1.4	404	108
24	0.000423	0.000024	0.282981	0.000026	241	7.4	12.5	0.9	375	72
25	0.000148	0.000008	0.282907	0.000041	225	4.8	9.9	1.5	477	114

*$t_{6/8}$ denotes the $^{206}Pb/^{238}U$ age for the same domain; $\varepsilon_{Hf}(t)$ is calculated assuming t to be metamorphic age that is derived from a weighted mean of U–Pb ages for each sample.

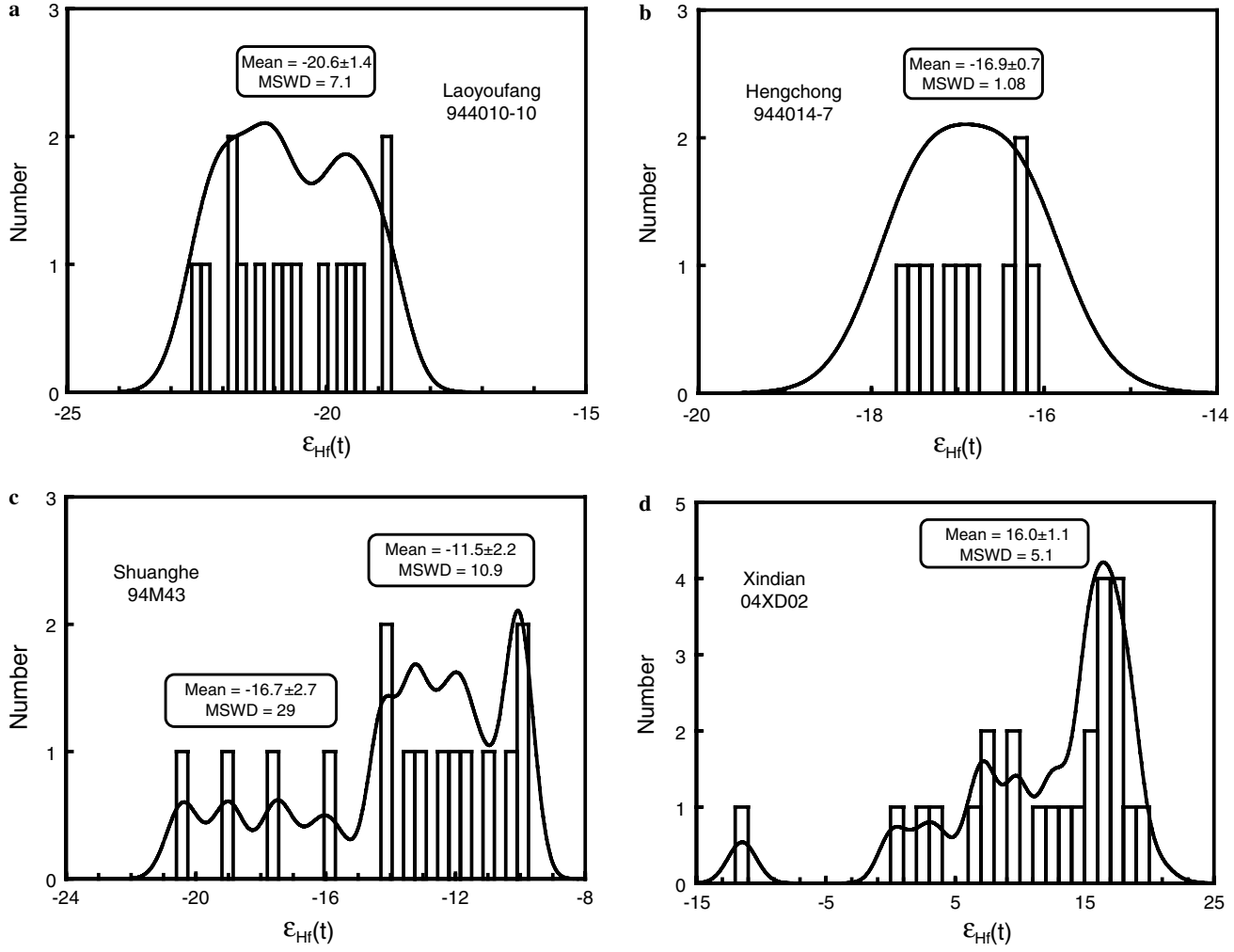

Fig. 4. Histograms of zircon $\varepsilon_{Hf}(t)$ values for eclogite enclosed in marble in the Dabie orogen. (a) Shima, (b) Hengchong, (c) Shuanghe, and (d) Xindian.

−13.4 to −9.8 with a weighted mean of -11.5 ± 2.2 (MSWD = 10.9) for the metamorphic domains (Fig. 4).

Twenty-five analyses for Lu–Hf isotope composition were made for 12 zircon grains from eclogite 04XD02 at Xindian (Table 3). Twenty-one analyses for the Triassic metamorphic domain show low $^{176}Lu/^{177}Hf$ ratios of 0.000003–0.000028 but high and variable $^{176}Hf/^{177}Hf$ ratios of 0.282631–0.283188. Assuming $t = 230$ Ma, calculated $\varepsilon_{Hf}(t)$ values vary from 0.1 to 19.8 (Table 3 and Fig. 4d). Except for four analyses giving low $\varepsilon_{Hf}(t)$ values, the other 17 analyses yield a weighted mean $\varepsilon_{Hf}(t)$ value of 16.0 ± 1.1 (MSWD = 5.1). However, the four analyses on the inherited core domains have high $^{176}Lu/^{177}Hf$ ratios of 0.000128–0.000341, with relatively low $^{176}Hf/^{177}Hf$ ratios of

0.282307–0.282905. At $t = 230$ Ma, calculated $\varepsilon_{Hf}(t)$ values are −11.4 to 9.8.

4.4. Mineral O isotopes

The O isotope compositions of mineral separates from the four eclogite samples are listed in Table 4. They have high $\delta^{18}O$ values of 12.3–16.0‰ for quartz, 9.9–21.4‰ for garnet, 7.9–21.9‰ for omphacite, 7.6–8.9‰ for biotite, 8.4‰ for rutile, 9.2‰ for titanite, 12.1‰ for calcite, and 16.9‰ for zircon. In sample 94M43, a $\delta^{18}O$ value of 7.9‰ for omphacite is significantly lower than that in equilibrium with quartz and garnet under eclogite-facies conditions, resulting in an unreasonably great fractionation of 4.4‰ between quartz and omphacite and even a negative fractionation of 2.0‰ between omphacite and garnet (Table 4). This is clearly a manifestation of O isotope disequilibria and thus indicates alteration of omphacite by retrograde metamorphism (Zheng et al., 1998b, 1999, 2002). In sample 04XD02, all minerals show obviously O isotope disequilibrium (Table 4), also testifying the effect of retrograde metamorphism. Except for these, calculated O isotope temperatures are 725–875 °C for quartz–garnet pairs, 650 °C for quartz–omphacite pairs, and 735–910 °C for garnet–omphacite pairs. It appears that these minerals have attained and preserved the high-T O isotope equilibrium under the eclogite-facies conditions. In contrast, low temperatures of 440–485 °C are calculated for the mineral pairs containing rutile and biotite, indicating that they experienced O isotope resetting by amphibolite-facies retrogression.

5. Discussion

5.1. Origin of high $\delta^{18}O$ eclogite

Except for sample 04XD02 and omphacite in sample 94M43, all the other eclogite minerals have attained and preserved high-T O isotope equilibrium. This indicates that high $\delta^{18}O$ values of 16.9–21.9‰ for garnet, omphacite and zircon (Table 4) are inherited from protolith of the eclogites. This type of high $\delta^{18}O$ eclogites was also reported in the Dabie-Sulu orogenic belt (Baker et al., 1997; Rumble et al., 2000; Chu et al., 2003; Zheng et al., 2003). Protolith of the marbles enclosing the eclogite lenses is the Neoproterozoic limestone that normally has very high $\delta^{18}O$ values of 18–25‰ (Rumble et al., 2000; Zheng et al., 2003). The high $\delta^{18}O$ eclogites and the host marbles have been show to approach oxygen isotope equilibrium on different scales (Rumble et al., 2000; Chu et al., 2003), with the highest $\delta^{18}O$ values for the eclogites similar to those of the marbles. These clearly indicate that the eclogite protoliths are sedimentary mudstone or volcano-sedimentary interlayer within the limestones and thus they are very rich in ^{18}O originally (Zheng et al., 2003). The large variations in $\delta^{18}O$ for the eclogites and their hosted marbles result from diagenesis, with local mixing of premetamorphic low $\delta^{18}O$ meteoric water with syn-deposition pore waters (Rumble et al., 2000).

The O isotope disequilibria between the coexisting minerals from eclogite 04XD02 and between omphacite and the other minerals from eclogite 94M43 are consistent with the petrographic observations that garnet and omphacite

Table 4
Oxygen isotope composition of minerals from eclogite within marble in the Dabie orogen

Sample No.	Mineral	$\delta^{18}O$ (‰)	Pair	$\Delta^{18}O$ (‰)	T (°C)[a]
944010	Quartz	15.98	Omp–Gt	0.81	735
Shima	Omphacite	13.56	Qz–Omp	2.42	650
	Garnet	12.75	Qz–Gt	3.23	725
	Rutile	8.42	Qz–Rt	7.56	440
944014-7	Omphacite	21.89			
Hengchong	Garnet	21.39	Omp–Gt	0.60	910
94M43	Quartz	12.34	Omp–Gt	−1.01	Disequilibrium
Shuanghe	Calcite	12.11	Qz–Cc	0.23	Equilibrium
	Omphacite	7.92	Qz–Omp	4.42	Disequilibrium
	Garnet	9.87	Qz–Gt	2.47	875
	Biotite	7.64	Qz–Bi	4.70	485
	Titanite	9.18	Qz–Tt	3.16	805
04XD02	Plagioclase	11.42			
Xindian	Muscovite	10.58	Pl–Mus	0.84	Disequilibrium
	Omphacite	9.94	Zr–Omp	6.91	Disequilibrium
	Garnet	12.64	Zr–Gt	4.21	Disequilibrium
	Zircon	16.85	Omp–Gt	−2.70	Disequilibrium
	Zoisite	12.66	Pl–Zs	−1.24	Disequilibrium
	Biotite	8.91	Pl–Bi	2.51	Disequilibrium
	Chlorite	8.39	Pl–Chl	3.03	Disequilibrium

[a] T was calculated by applying the calibrations of Zheng (1993a,b); judgement of equilibrium or disequilibrium also follows the calibrations together with previous studies of oxygen isotopes in eclogite minerals (Zheng et al., 1999, 2002).

are partly replaced by amphibolite-facies symplectite composed of amphibole + plagioclase and that rutile is partly transformed into titanite. These appear to be evidence for late fluid-assisted retrogression. Nevertheless, retrograde fluids are internally buffered in O isotope composition, so that the high $\delta^{18}O$ values are principally retained for the eclogite minerals and thus can still be used to decipher their protolith nature.

Because eclogite-facies metamorphism can enhance the $\varepsilon_{Hf}(t)$ values of newly grown zircon by 3.1–13.5 and thus reduce zircon Hf model ages (Zheng et al., 2005a), T_{DM1} ages listed in Table 3 cannot provide quantitative constraints on protolith ages of the marble-hosted eclogites. Nevertheless, sample 04XD02 at Xindian show positive $\varepsilon_{Hf}(t)$ values of 16.0 ± 1.1 for most of analyses, which are markedly different from the negative $\varepsilon_{Hf}(t)$ values of -20.6 ± 1.4 to -11.5 ± 2.2 for the other three samples (Fig. 4). This clearly indicates that protolith of eclogite 04XD02 is more juvenile than the others even if taking into account the metamorphic effect. Thus this eclogite protolith may originate from the volcano-sedimentary interlayer that formed by rift volcanism during breakup of the supercontinent Rodinia (Zheng et al., 2004, 2006). In contrast, the negative $\varepsilon_{Hf}(t)$ values for the other three eclogites correspond to the protolith of sedimentary mudstone that was derived from weathered ancient crust (Paleoproterozoic?). The presence of a few negative $\varepsilon_{Hf}(t)$ values for eclogite 04XD02 also indicates minor contributions from the old crust, consistent with the occurrence of inherited zircons that show two groups of U–Pb age at 812 ± 30 Ma and 1806 ± 32 Ma, respectively (Fig. 3d).

5.2. Genesis of metamorphic zircons

Metamorphic zircon can form by either recrystallization of preexisting zircon or growth in the presence of fluid. Because of its resistant nature with very low rates of Pb diffusion (Cherniak and Watson, 2003), crystalline zircon is capable of recording the time at which it grew during igneous and metamorphic processes. In contrast, metamict zircon is susceptible to metamorphic recrystallization and thus to complete resetting of U–Pb radiometric system (Cherniak and Watson, 2003). As a result, the completely recrystallized zircon can provide record for timing of metamorphic resetting in the presence of fluid. Therefore, the geological interpretation of zircon U–Pb ages is relevant to the formation mechanism of metamorphic zircon and fluid availability.

Because Hf and Zr have geochemical affinities to each other, zircon usually has very high Hf content (from 0.5% to >1%), and thus very low Lu/Hf ratio (usually <0.0005). In contrast, other REE-rich minerals such as garnet, monazite, allanite, xenotime and apatite generally have high Lu/Hf ratios (Kinny and Maas, 2003; Zheng et al., 2005a). In a closed system where zircon grew from its matrix, it is expected to have a great difference in Lu/Hf ratio between zircon and these minerals, and their Hf isotope compositions will evolve in different ways (Amelin et al., 2000). After sometime later when new zircon grew by breakdown and recrystallization of these REE-rich minerals, it would incorporate the Hf isotopic compositions of coexisting minerals, and thus has different $^{176}Hf/^{177}Hf$ ratios for different grains and/or domains. The metamorphic zircons with the high $^{176}Hf/^{177}Hf$ ratios indicate their growth by the breakdown and recrystallization of high Lu/Hf minerals (Zheng et al., 2005a). On the other hand, the metamorphic zircons with the low $^{176}Hf/^{177}Hf$ ratios may principally reflect the Lu–Hf isotope features of their host rocks. The breakdown of low Lu/Hf minerals could occur during the zircon growth, possibly with the Ostwald ripening as the mechanism for overgrowth (Ayers et al., 2003).

Three mechanisms can be considered for zircon growth during high-grade metamorphism: (1) crystallization from melt during anatexis (Roberts and Finger, 1997; Vavra et al., 1999; Keay et al., 2001); (2) nucleation and crystallization due to Zr and Si release by metamorphic breakdown reactions of minerals under subsolidus to solidus conditions (Fraser et al., 1997; Bingen et al., 2001); (3) growth in the presence of aqueous fluids (Liati and Gebauer, 1999; Rubatto et al., 1999; Vavra et al., 1999; Rubatto and Hermann, 2003; Dubinskaa et al., 2004), with overgrowth often by Ostwald ripening (Ayers et al., 2003). Different kinds and origins of fluid could be involved in these mechanisms, including CO_2-bearing fluid from the marble, H_2O-rich fluid from inside the eclogite lens, internally derived fluid from the decomposition of hydrous minerals and the exsolution of structural hydroxyl from nominally anhydrous minerals, and externally derived fluid flushing the whole system. So far no evidence for anatectic process has been found in our samples and other petrological studies (Xu et al., 1992; Okay, 1993; Schertl and Okay, 1994; Cong, 1996; Zhang and Liou, 1996; Carswell et al., 1997), thus the first mechanism can be precluded at first.

Under the conditions of amphibolite-facies, eclogite-facies and granulite-facies metamorphism, there are abundant metamorphic garnets to form and recrystallize. Omphacite is a characteristic mineral of eclogite-facies metamorphism. Both garnet and omphacite have been demonstrated to be the major minerals containing Zr in UHP eclogites (Sassi et al., 2000). Although breakdown of the two minerals could result in zircon growth during eclogite-facies recrystallization, no significant growth can occur in the absence of fluid (Fraser et al., 1997; Zheng et al., 2004). As pointed out by Corfu et al. (2003), all metamorphic zircon growth (and resorption) occurs only in the presence of a fluid phase. Thus the fluid-absent growth can be excluded by the morphological observations that our metamorphic zircons have the large sizes and volumes (Fig. 2). In this regard, the second mechanism requires the presence of metamorphic fluid and hence is consistent with fluid-assisted growth in the third mechanism. Therefore, the growth of metamorphic zircon was finally related to fluid availability during high-grade metamorphism. The

sedimentary protolith for our eclogites is capable of providing sufficient fluids for growth of metamorphic zircon during both subduction and exhumation of continental crust. The appearance of resorption structures (Fig. 2) also suggests that the fluid was present during the formation of these metamorphic zircons. Nevertheless, it remains to resolve what kind of fluids (CO_2 versus H_2O) was present during the eclogite-facies metamorphism.

In our four samples of eclogite, most of the zircons show irregular shape, anhedral with internal structures of variable zoned or unzoned (Fig. 2), and have low Th/U ratios (Tables 1 and 2). These features are generally ascribed to metamorphically grown zircons in high-grade metamorphic rocks (Hoskin and Black, 2000; Tomaschek et al., 2003; Bingen et al., 2004). The U–Pb dates yield the two groups of age at 245 ± 3 to 240 ± 2 Ma and 226 ± 4 to 223 ± 2 Ma, respectively (Fig. 3), corresponding to two episodes of zircon growth during the Triassic continental collision. It is interesting to note that the Lu–Hf isotopic analyses show two subgroups for the metamorphic zircons (Table 3): (1) low $^{176}Lu/^{177}Hf$ but high $^{176}Hf/^{177}Hf$ ratios, (2) high $^{176}Lu/^{177}Hf$ and high $^{176}Hf/^{177}Hf$ ratios. This difference may be used to indicate the growth mechanism of metamorphic zircons.

Most of the metamorphic zircons exhibit the very low $^{176}Lu/^{177}Hf$ ratios of 0.000001–0.000024 but relatively higher $\varepsilon_{Hf}(t)$ values (Table 3). This indicates that there was the concurrent formation of HREE-enriched minerals with the metamorphic zircons (Degeling et al., 2001; Bingen et al., 2004; Zheng et al., 2005a). Since garnet is a major mineral that intensively incorporates HREE, either crystallization or recrystallization of garnet during high-grade metamorphism can result in HREE depletion for the concurrently formed minerals (Rubatto, 2002; Rubatto and Hermann, 2003; Whitehouse and Platt, 2003; Zheng et al., 2005a). Because the UHP eclogite-facies metamorphism only involves the internally derived fluid from the decomposition of hydrous minerals and the exsolution of hydroxyl from nominally anhydrous minerals (Zheng et al., 2003), the change in zircon $^{176}Lu/^{177}Hf$ ratio could reflect the source of fluid that either was itself Lu depleted or contained minerals like garnet that sequestered Lu. In either case, the low $^{176}Lu/^{177}Hf$ ratios for the metamorphically grown zircons attest their contemporaneous formations with garnet. Nevertheless, it remains to resolve whether it is Lu depletion or Hf enrichment results in the reduction in zircon Lu/Hf ratios for our samples.

Analysis #1 for metamorphic zircon in sample 944010-10 shows a high $^{176}Lu/^{177}Hf$ ratio of 0.000383 (Table 3). Three analyses for the metamorphic zircon in sample 944014-7 (spots #4, #5 and #6) also yield the relatively high $^{176}Lu/^{177}Hf$ ratios of 0.000186–0.000251 (Table 3). They are all about two orders of magnitude higher than those of the remaining metamorphic zircons in the same samples. As revealed by the CL images (237.3 Ma spot in Figs. 2a and 243.8 Ma spot in Fig. 2b), these zircons have different features of surface and internal structures from the other metamorphic zircons, suggesting that they probably formed in distinct environments. If no precipitation of garnet would coevally occur during high-grade metamorphism, the high Lu/Hf zircons could form either by complete recrystallization of igneous protolith zircons with high Lu/Hf ratios or by growth from locally high Lu/Hf fluids, whereas the low Lu/Hf zircons would form by growth from locally low Lu/Hf fluids. Because the presence or absence of garnet dictates the $^{176}Lu/^{177}Hf$ ratios of contemporaneously grown zircon, the high Lu/Hf ratios in our metamorphic zircons suggest their formation in the presence of high Lu/Hf fluid prior to the appearance of garnet.

In samples 944010-10 and 944014-7, the two subgroups of metamorphic zircons have the similar $^{176}Hf/^{177}Hf$ ratios despite the significant difference in their $^{176}Lu/^{177}Hf$ ratio (Table 3 and Fig. 4). The metamorphic zircons of high Lu/Hf ratios are demonstrated to grow prior to the appearance of garnet, and thus a little earlier than the other metamorphic zircons of low Lu/Hf ratios in the same sample that formed concurrently with garnet despite the indistinguishable U–Pb ages between them. Nevertheless, there was no substantial change in Hf isotope composition during the two types of metamorphic zircon growth.

The metamorphic zircons in samples 94M43 and 04XD02 can be divided into the two groups based on their U–Pb ages (ca. 240 Ma and ca. 225 Ma in Fig. 3) and/or internal structures of mantle and rim (Fig. 2). The Lu–Hf isotope compositions for the two groups of zircons in 94M43 are similar to each other, indicating that the two episodes of fluid-assisted zircon growth have the identical characteristics of Hf isotopes. On the other hand, most of the metamorphic zircons in sample 04XD02 have the high $\varepsilon_{Hf}(t)$ values of 9.8–18.8, but a few ca. 240 Ma zircons show the very low $\varepsilon_{Hf}(t)$ values of 0.1–7.3 (Table 3). This indicates that a few old inherited zircons were involved in the zircon formation.

In sample 94M43, the inherited cores show no or weak zoning with the relatively strong or weak brightness and resorption structures in CL images (Fig. 2c); the five inherited cores have the discordant U–Pb ages but are distributed along the discordia line (Fig. 3c). This indicates that the inherited zircons experienced different degrees of metamorphic recrystallization in the presence of fluid (Zheng et al., 2004, 2005a). They have the higher $^{176}Lu/^{177}Hf$ ratios but lower $^{176}Hf/^{177}Hf$ ratios than those of the metamorphically overgrown domains (Table 3). The all analyses show a positive correlation between $^{206}Pb/^{238}U$ age and $^{176}Lu/^{177}Hf$ ratio (Fig. 5a) but a negative correlation between $^{206}Pb/^{238}U$ age and $^{176}Hf/^{177}Hf$ ratio (Fig. 5b). It appears that the UHP eclogite-facies metamorphism results in increased $^{176}Hf/^{177}Hf$ ratios for the metamorphically grown zircons. The similar observations are also obtained from zircons in eclogite 04XD02 at Xindian (Fig. 6b) and UHP eclogite-facies metagranite and metabasite in the Dabie orogen (Zheng et al., 2005a), indicating the identical effect on both Lu–Hf and U–Th–Pb isotope systems by metamorphic recrystallization in the presence of fluid. It

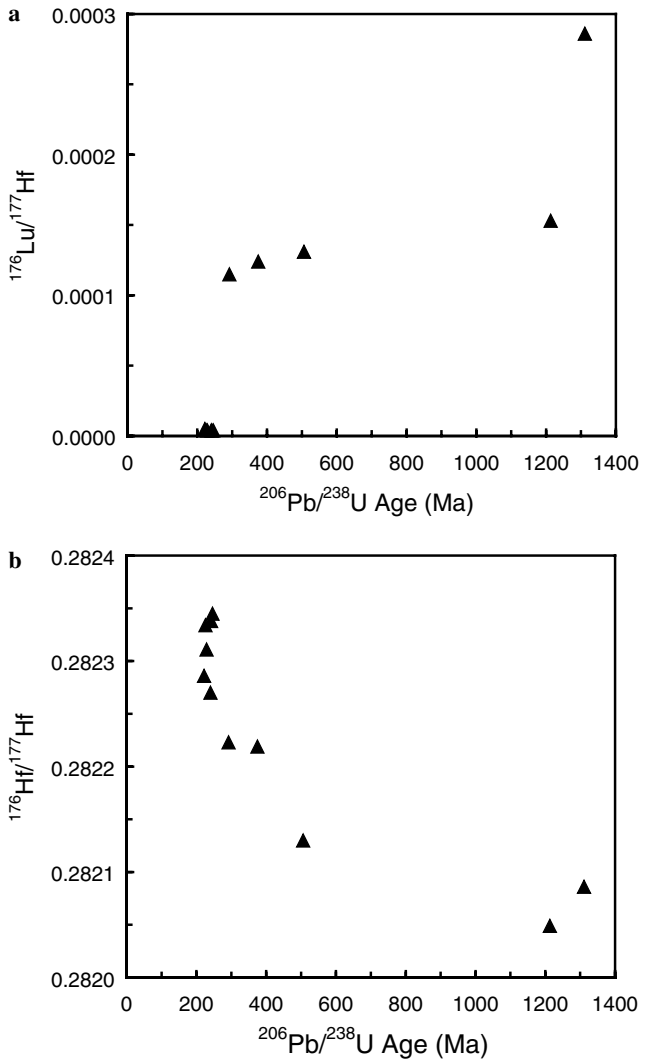

Fig. 5. Plots of $^{206}Pb/^{238}U$ age versus $^{176}Lu/^{177}Hf$ or $^{176}Hf/^{177}Hf$ ratio for zircon in eclogite 94M43 at Shuanghe in the Dabie terrane. (a) $^{206}Pb/^{238}U$ age versus $^{176}Lu/^{177}Hf$ ratio, and (b) $^{206}Pb/^{238}U$ age versus $^{176}Hf/^{177}Hf$ ratio.

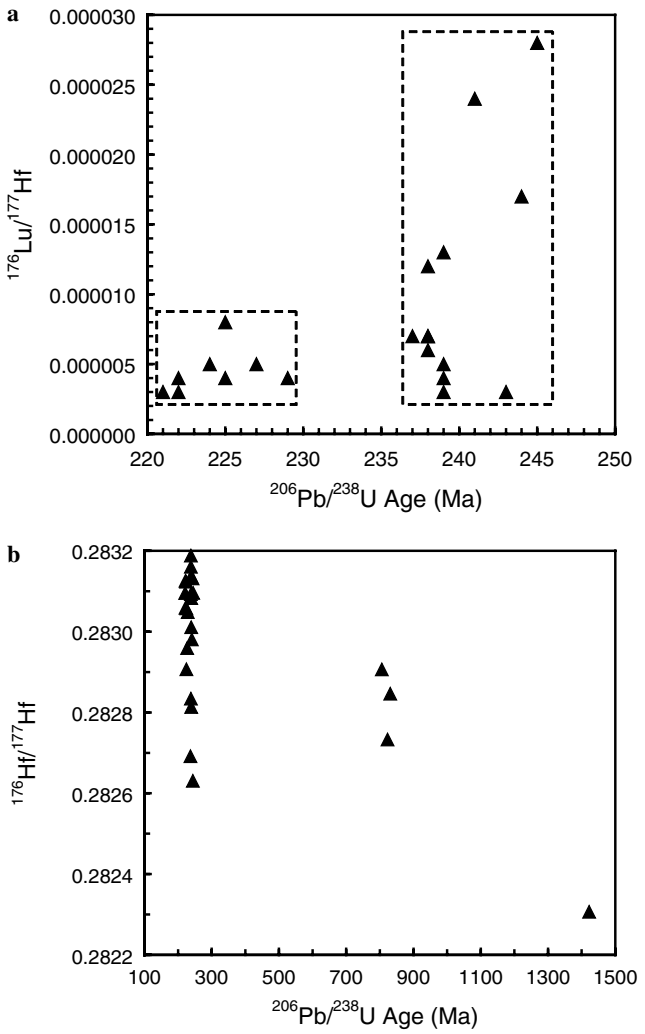

Fig. 6. Plot of $^{206}Pb/^{238}U$ age versus $^{176}Lu/^{177}Hf$ or $^{176}Hf/^{177}Hf$ ratio for metamorphic zircon in eclogite 04XD02 at Xindian in the Dabie orogen. (a) $^{206}Pb/^{238}U$ age versus $^{176}Lu/^{177}Hf$ ratio, and (b) $^{206}Pb/^{238}U$ age versus $^{176}Hf/^{177}Hf$ ratio.

is known that low Th and low LREE contents of metamorphic zircon are related to coeval crystallization of epidote-group minerals under fluid-present eclogite-facies conditions (e.g., Bingen et al., 2004). Microscopic observations do show the heterogeneous occurrence of zoisite or epidote in our eclogite samples. Thus coeval recrystallization of garnet and epidote-group minerals can be used to explain the correlated variations between $^{206}Pb/^{238}U$ age and $^{176}Hf/^{177}Hf$ ratio.

The $^{176}Lu/^{177}Hf$ ratios for the first age group of metamorphic zircons in sample 04XD02 are higher and more variable than those for the second age group (Fig. 6a). As demonstrated by Rayleigh fractionation model (Lapen et al., 2003), garnet incorporates the majority of available HREE and Y in is early growth stage, and consequently show large variation/zoning in HREE contents. Zircon also partition HREE. Correspondingly, zircon grown concurrently with the early stage of garnet growth has high and variable HREE contents, and thus has comparatively high $^{176}Lu/^{177}Hf$ ratios. So, the first age group of metamorphic zircon reported in this study, crystallized between 245 ± 3 and 240 ± 2 Ma, and characterized by $^{176}Lu/^{177}Hf$ ratios of 0.000192–0.000383, probably corresponding to zircon formed during the prograde stage of HP-UHP metamorphism when garnet started to grow in the presence of a fluid phase.

The large variations in $\varepsilon_{Hf}(t)$ for the metamorphic zircons occur not only within the individual samples but also in the region in the eastern part of the Central Dabie zone (Fig. 4). While the UHP eclogite-facies metamorphism can increase the $\varepsilon_{Hf}(t)$ values of newly grown zircon (Zheng et al., 2005a), protolith nature of eclogites also dictates their initial Hf isotope ratios. The occurrence of both negative and positive $\varepsilon_{Hf}(t)$ values for the zircons suggest that both ancient and juvenile crusts were involved in formation of their protoliths (Zheng et al., 2006). In particular, the combined study of zircon Hf–O isotopes indicates that

the negative $\varepsilon_{Hf}(t)$ eclogites have their protolith derived from the sedimentary mudstone of ancient crustal source, whereas the positive $\varepsilon_{Hf}(t)$ eclogite has its protolith originating from the volcano-sedimentary interlayer of juvenile crustal source. In either case, metamorphic zircon grew significantly due to the presence of fluid, leaving the occurrence of no or minor detrital or inherited zircon. Nevertheless, preservation of the large variations in the initial Hf isotope ratios (Fig. 4) indicates very limited homogenization of Hf isotopes by the UHP eclogite-facies metamorphism even if the fluid was available for zircon growth.

5.3. Timing of metamorphic zircon growth

A great progress has been made lately by means of SHRIMP U–Pb dating on coesite-bearing domains of metamorphic zircon from UHP metamorphic rocks in the Dabie-Sulu orogenic belt. The results show two groups of Triassic age: (1) 243 ± 1 Ma for jadeite quartzite (Liu and Jian, 2004), 244 ± 5 Ma for granitic gneiss (Wan et al., 2005), and 245 ± 14 Ma for granitic gneiss (Liu et al., 2005); (2) 228 ± 2 Ma for the jadeite quartzite (Liu and Jian, 2004), 234 ± 4 Ma (Liu and Xu, 2004), 231 ± 4 Ma (Liu et al., 2004a), 227 ± 2 Ma (Liu et al., 2004b), and 226 ± 2 Ma (Wan et al., 2005) for granitic gneiss, and 227 ± 5 Ma for amphibolized peridotite (Yang et al., 2003). It appears that there are the two episodes of zircon growth in the field of coesite stability during the Triassic UHP metamorphism. In particular, the Early Triassic ages of 245–240 Ma were principally obtained from the metasedimentary rocks such as jadeite quartzite (Ayers et al., 2002; Liu and Jian, 2004), paragneiss (Liu et al., 2005), and marble-associated eclogite (this study) as well as low-T/UHP eclogite whose protolith is a kind of altered basalts (Li et al., 2004).

In high-grade metamorphic rocks, fluid availability plays a critical role in dictating zircon growth or overgrowth (Rubatto et al., 1999; Ayers et al., 2002; Corfu et al., 2003; Schersten et al., 2004; Zheng et al., 2004, 2005a). For the Dabie-Sulu UHP metamorphic rocks, the SHRIMP zircon U–Pb dating for coesite-bearing domains reveals episodic growth of metamorphic zircons at 242 ± 2 Ma and 227 ± 2 Ma (Fig. 7), with an interval at about 240–235 Ma (Ayers et al., 2002; Li et al., 2004; Liu and Xu, 2004; Liu et al., 2004a,b, 2005; Liu and Jian, 2004; Wan et al., 2005; Zheng et al., 2005a). It appears that there was fluid unavailability for zircon growth under the peak UHP conditions during the Middle Triassic. This is consistent with the systematic studies of stable isotopes and fluid inclusions in eclogite minerals from the Dabie-Sulu orogenic belt, which demonstrate that fluid flow is very limited in the peak UHP stage (Rumble et al., 2000; Fu et al., 2001; Zheng et al., 2003). Thus no detectable growth of zircon occurred at the peak of UHP metamorphism. Instead, the zircon is able to grow in the presence of metamorphic fluid that was released by a pressure increase from coesite phase to diamond phase during the final subduction and by a pressure decrease from diamond phase to coesite phase during early exhumation. Therefore, the two episodes of zircon growth in the field of coesite stability may suggest the two pulses of fluid availability at 242 ± 2 Ma and 227 ± 2 Ma, respectively, prior to the onset of and shortly following the pressure climax in the UHP regime (Fig. 8).

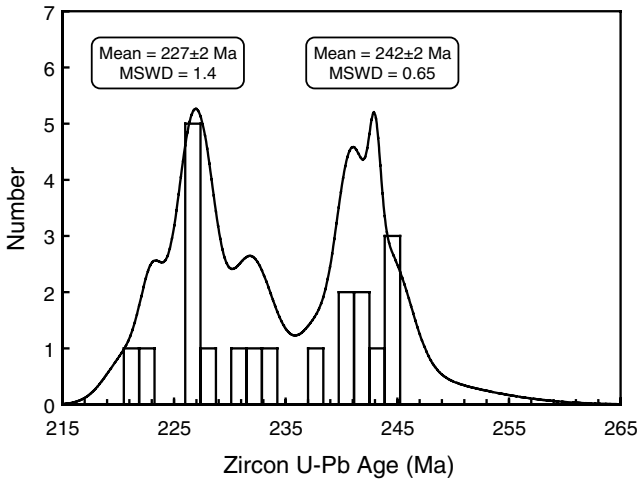

Fig. 7. Cumulative probability plot of zircon U–Pb ages for coesite-bearing domains (Yang et al., 2003; Liu and Jian, 2004; Liu and Xu, 2004; Liu et al., 2004a,b, 2005; Wan et al., 2005) and other studies concerning mineral paragenesis of coesite occurrence (Ayers et al., 2002; Li et al., 2004; Zheng et al., 2005a; this study). Two episodes of zircon growth in the field of coesite stability statistically cluster at 242 ± 2 Ma and 227 ± 2 Ma, respectively, corresponding to two pulses of fluid availability in the ultrahigh-pressure regime.

The occurrence of coesite was universally identified in metamorphic minerals from the three types of eclogite in the Dabie-Sulu orogenic belt, demonstrating metamorphic conditions at >2.8 GPa at 700–800 °C. Microdiamond was also found in some of coesite-bearing eclogites (Xu et al., 1992, 2003, 2005), indicating peak pressures as high as 3.6 GPa at 750 °C. It is possible that the maximum temperatures were attained at pressures well below those required for diamond stability during the prograde UHP metamorphism, and that an early part of the exhumation history was accomplished under near-isothermal conditions (e.g., Carswell and Zhang, 1999; Zheng et al., 2002; Wan et al., 2005). For this reason, Zheng et al. (2005a) interpreted the two group U–Pb ages as recording the two episodes of zircon growth or overgrowth, respectively, prior to the peak pressure during the late subduction (a transition from HP to UHP eclogite-facies) and subsequent to the peak temperature during the initial exhumation (a transition from UHP to HP eclogite-facies). By integrating all available dates for zircon growth and metamorphic P-T conditions, schematic P-T-t path is constructed in Fig. 8 for metamorphic zircon growth in the Dabie-Sulu orogenic belt. The prograde UHP growth at 242 ± 2 Ma may occur at about 600–750 °C and 2.0–3.0 GPa, whereas the

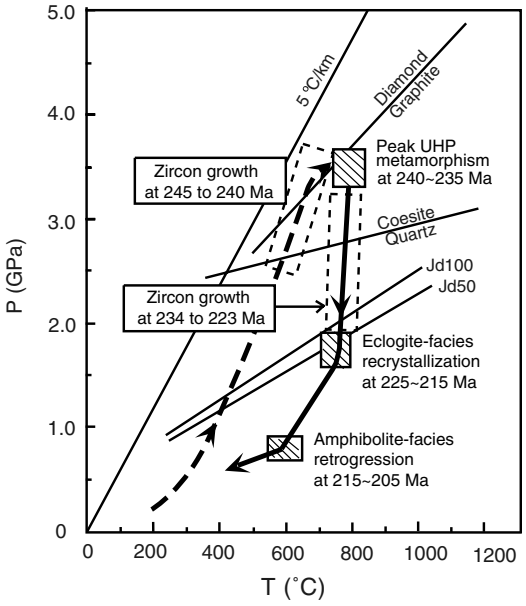

Fig. 8. Schematic P-T-t path for ultrahigh-pressure metamorphism in the Dabie-Sulu orogenic belt, with fluid availability for zircon growth at 245–240 Ma and 234–223 Ma, respectively, prior to the onset of and subsequent to the peak pressure. Zircon U–Pb ages used to construct this path include SHRIMP dating on coesite-bearing domains (Yang et al., 2003; Liu and Jian, 2004; Liu and Xu, 2004; Liu et al., 2004a,b, 2005; Wan et al., 2005) and other studies concerning mineral paragenesis of coesite occurrence (this study; Ayers et al., 2002; Li et al., 2004; Zheng et al., 2005a). Dashed framework denote the P-T-t path for two episodes of zircon growth, respectively, prior to the onset of prograde UHP event during the deep subduction and subsequent to the pressure decrease from diamond phase through coesite phase to the HP eclogite-facies regime during the early exhumation.

retrograde UHP growth at 227 ± 2 Ma may occur at about 750–650 °C and 3.6–2.4 GPa. Furthermore, retrograde growth at HP eclogite-facies may occur at 220 ± 5 Ma at about 750–650 °C and 2.4–1.6 GPa, and retrograde growth at amphibolite-facies may occur at 210 ± 5 Ma at about 650–550 °C and 1.6–0.8 GPa.

During the prograde HP and UHP metamorphism, the decomposition of hydrous minerals such as paragonite (Li et al., 2004), chlorite (Fraser et al., 2004), biotite (Vavra et al., 1999), serpentine (Früh-Green et al., 2001), glaucophane (Rubatto et al., 1999), and amphibole (Fraser et al., 1997) is expected to release aqueous fluids at temperatures of 500–700 °C. These fluids may become focused during the transition of metamorphic reactions from the HP to UHP phases and from the coesite to diamond stability fields, resulting in the zircon growth at the Early Triassic (this study; Wan et al., 2005; Liu et al., 2005; Liu and Jian, 2004). As documented before for the metamorphic zircons of Early Triassic ages in our marble-hosted eclogites, the zircons with the high Lu/Hf ratios and high $\varepsilon_{Hf}(t)$ values grew prior to the appearance of garnet. They are only slightly older than, but indistinguishable from, the zircons that have the low Lu/Hf ratios and low $\varepsilon_{Hf}(t)$ values in the same sample and thus grew concurrently with garnet. In this regard, the first age group of 245 ± 3 to 240 ± 2 Ma for our metamorphic zircons (Fig. 3) may date their growth in the prograde HP to UHP stage (Fig. 8), during which there is a transition from no appearance of garnet to the initial growth of garnet with fluid availability. Sufficient fluid was available for the zircon growth by dehydration of HP metasedimentary rocks at the late stage of deep subduction.

On the other hand, the inclusions of aqueous fluid (H_2O) were detected from metamorphic zircon domains containing UHP minerals (such as coesite and low Al_2O_3 enstatite) with U–Pb ages of 226–220 Ma (Liu and Xu, 2004; Zhang et al., 2005), indicating the presence of aqueous fluid in the retrograde stage from the diamond to coesite stability fields during the early exhumation. Breakdown of hydrous minerals such as lawsonite (Li et al., 2004) and decompression exsolution of hydroxyl dissolved in such nominally anhydrous minerals as garnet and omphacite (Zheng et al., 1999, 2003) have been suggested to provide significant amounts of the aqueous fluid for the second episode of zircon growth during exhumation. This can also cause the extensive recrystallization, retrograde alteration and even quartz veining (Zheng et al., 2003). As a result, the abundant U–Pb ages of Late Triassic may record the timing of HP retrogression downward from the UHP metamorphic regime. Obviously, sufficient fluid became available again for the zircon growth or overgrowth by dehydration of both UHP metasedimentary and metaigneous rocks during the exhumation.

On the basis of internal structure, U–Pb ages and Lu–Hf isotope compositions for metamorphic zircons in this study as well as the previous age results (Rowley et al., 1997; Hacker et al., 1998; Ayers et al., 2002; Liu and Jian, 2004; Liu and Xu, 2004; Liu et al., 2004a,b, 2005; Zheng et al., 2004, 2005a; Wan et al., 2005), we suggest that the two groups of zircon U–Pb age may probably date two episodes of zircon growth, respectively, prior to the onset of prograde UHP event during the deep subduction and subsequent to the pressure decrease from diamond phase through coesite phase to the HP eclogite-facies regime during the early exhumation (Fig. 8). In particular, the two groups of zircon U–Pb age for the UHP metasedimentary rocks place important constraints on timing of the two episodes of fluid availability, respectively, in the process of prograde HP to UHP transition during the deep subduction and in the process of retrograde UHP to HP transition during the early exhumation. Furthermore, timescale of UHP metamorphism in the Dabie-Sulu orogenic belt is geochronologically constrained to be about 11–19 Ma (a difference between 242 ± 2 Ma and 227 ± 2 Ma by taking into account the uncertainty in both ages), probably lasting for 15 ± 2 Ma in the field of coesite stability. This lends support to previous estimates by mineral O isotope studies that suggest a short duration of 5–10 Ma for the peak UHP metamorphism occurred in (Zheng et al., 1998b), but an order of 10–20 Ma for bulk recycling of continental subduction, UHP metamorphism at mantle and exhumation (Zheng et al., 2003).

6. Conclusions

The presence of fluids enables zircon growth in UHP metamorphic rocks during subduction and exhumation of continental crust. Metamorphic zircons from UHP eclogites and gneisses in the Dabie-Sulu orogenic belt occur in two types: metamorphically grown and recrystallized ones. Triassic U–Pb ages for zircon growth are further subdivided into two groups at 242 ± 2 Ma and 227 ± 2 Ma, respectively. They are interpreted as the ages of two episodes of fluid availability, respectively, at the onset of prograde transition from HP to UHP during deep subduction and at the retrograde transition from UHP to HP regimes during early exhumation. Thus timescale of UHP metamorphism is constrained to be about 11–19 Ma, probably 15 ± 2 Ma for the persistence of ultrahigh pressures in the field of coesite stability. Protoliths of marble-hosted eclogite are sedimentary mudstone or volcanosedimentary interlayer within the limestone, which may contain sufficient amounts of fluid available for zircon growth during the continental subduction-zone metamorphism. Most of the metamorphically grown zircons have very low Lu/Hf ratios, indicating their crystallization in the presence of garnet under HP eclogite-facies conditions. A few of the first episode zircons have higher and more variable Lu/Hf ratios, suggesting their formation before the appearance of garnet. Thus the first episode of metamorphic zircon growth is correlated with fluid availability during the prograde HP-UHP stage prior to the onset of peak UHP metamorphism, whereas the second episode of zircon growth is associated with fluid availability during the retrograde UHP-HP metamorphism subsequent to the peak UHP regime. Therefore, the Lu–Hf isotope system of metamorphically grown zircons can place geochemical constraints on the growth mechanism of metamorphic zircons.

Acknowledgments

This study was supported by the Natural Science Foundation of China (40573011), the Natural Science Key Project of Universities in Anhui Province (2006KJ046A) and the National Ministry of Science and Technology (2003CB716501). Thanks are due to Dr. Yunuo Shi for their assistance with SHRIMP zircon U–Pb dating, to Mr. Zhengyu Chen for their assistance with CL imaging, and to Dr. Liewen Xie for their assistance with LA-MC-ICPMS zircon Hf isotope analysis. Comments by Y. Amlin, T. Andersen, B. Bingen and an anonymous reviewer have greatly helped improvement of the manuscript.

Associate editor: Yuri Amelin

References

Ames, L., Zhou, G.Z., Xiong, B.C., 1996. Geochronology and isotopic character of ultrahigh-pressure metamorphism with implications for collision of the Sino-Korean and Yangtze cratons, central China. *Tectonics* **15**, 472–489.

Amelin, Y., Lee, D.C., Halliday, A.N., 2000. Early-middle Archean crustal evolution deduced from Lu–Hf and U–Pb isotopic studies of single zircon grains. *Geochim. Cosmochim. Acta* **64**, 4205–4225.

Andersen, T., 2002. Correction of common lead in U–Pb analyses that do not report ^{204}Pb. *Chem. Geol.* **192**, 59–79.

Ayers, J.C., Dunkle, S., Gao, S., Miller, C.F., 2002. Constraints on timing of peak and retrograde metamorphism in the Dabie Shan Ultrahigh-Pressure Metamorphic Belt, east-central China, using U–Th–Pb dating of zircon and monazite. *Chem. Geol.* **186**, 315–331.

Ayers, J.C., Delacruz, K., Miller, C., Switzer, O., 2003. Experimental study of zircon coarsening in quartzite $\pm H_2O$ at 1.0 GPa and 1000 °C, with implications for geochronological studies of high-grade metamorphism. *Am. Mineral.* **88**, 365–376.

Baker, J., Mathews, A., Mattey, D., Rowley, D., Xue, F., 1997. Fluid-rock interactions during ultra-high pressure metamorphism, Dabie Shan, China. *Geochim. Cosmochim. Acta* **61**, 1685–1696.

Bingen, B., Austrheim, H., Whitehouse, M.J., 2001. Ilmenite as a source for zirconium during high-grade metamorphism? Textural evidence from the Caledonides of Western Norway and implications for zircon geochronology. *J. Petrol.* **42**, 355–375.

Bingen, B., Austrheim, H., Whitehouse, M.J., Davis, W.J., 2004. Trace element signature and U–Pb geochronology of eclogite-facies zircon, Bergen Arcs, Caledonides of W Norway. *Contrib. Mineral. Petrol.* **147**, 671–683.

Black, L.P., Kamob, S.L., Allenc, C.M., Aleinikoffd, J.N., Davisb, D.W., Korscha, R.J., Foudoulisa, C., 2003. TEMORA 1: a new zircon standard for Phanerozoic U–Pb geochronology. *Chemical Geol.* **200**, 155–170.

Blichert-Toft, J., Albarede, F., 1997. The Lu–Hf geochemistry of chondrites and the evolution of the mantle-crust system. *Earth Planet. Sci. Lett.* **148**, 243–258, Erratum, 154, 349.

Brueckner, H.K., Blusztajn, J., Bakun-Czubarow, N., 1996. Trace element and Sm-Nd "age" zoning in garnets from peridotites of the Caledonian and Variscan Mountains and tectonic implications. *J. Metamorph. Geol.* **14**, 61–73.

Carswell, D.A., O'Brien, P.J., Wilson, R.N., Zhai, M.G., 1997. Thermobarometry of phengite-bearing eclogites in the Dabie Mountains of central China. *J. Metamor. Geol.* **15**, 239–252.

Carswell, D.A., Zhang, R.Y., 1999. Petrographic characteristics and metamorphic evolution of ultrahigh-pressure eclogites in plate-collision belts. *Intern. Geol. Rev.* **41**, 781–798.

Cherniak, D.J., Watson, E.B., 2003. Diffusion in zircon. *Rev. Mineral. Geochem.* **53**, 113–143.

Chu, N.C., Taylor, R.N., Chavagnac, V., Nesbitt, R.W., Boella, R.M., Milton, J.A., Germain, C.R., Bayon, G., Burton, K., 2002. Hf isotope ratio analysis using multi-collector inductively coupled plasma mass spectrometry: an evaluation of isobaric interference corrections. *J. Anal. Atom. Spectrom.* **17**, 1567–1574.

Chu, X.-L., Guo, J.-H., Fan, H.-R., Jin, C.-W., 2003. Oxygen isotope compositions of eclogites in Rongcheng, Eastern China. *Chinese Sci. Bull.* **48**, 372–378.

Cong, B.-L., 1996. *Ultrahigh-Pressure Metamorphic Rocks in the Dabie-shan-Sulu Region of China*. Science Press, Beijing, p. 224.

Corfu, F., Hanchar, J.M., Hoskin, P.W.O., Kinny, P., 2003. Altas of zircon textures. *Rev. Mineral. Geochem* **53**, 469–500.

DeBievre, P., Taylor, P.D.P., 1993. Table of the isotopic composition of the elements. *Int. J. Mass. Spectrom. Ion Process.* **123**, 149.

Degeling, H., Eggins, S., Ellis, D.J., 2001. Zr budgets for metamorphic reactions, and the formation of zircon from garnet breakdown. *Mineral. Mag.* **65**, 749–758.

Dubinskaa, E., Bylinab, P., Kozlowskia, A., Dorric, W., Nejbertd, K., Schastokc, J., Kulickie, C., 2004. U–Pb dating of serpentinization: hydrothermal zircon from a metasomatic rodingite shell (Sudetic ophiolite, SW Poland). *Chem. Geol.* **203**, 183–203.

Fan, W.M., Guo, F., Wang, Y.J., Zhang, M., 2004. Late Mesozoic volcanism in the northern Huaiyang tectono-magmatic belt, central

China: partial melts from a lithospheric mantle with subducted continental crust relicts beneath the Dabie orogen? *Chem. Geol.* **209**, 27–48.

Fraser, G., Ellis, D., Eggins, S., 1997. Zirconium abundance in granulite-facies minerals, with implications for zircon geochronology in high-grade rocks. *Geology* **25**, 607–610.

Fraser, G., Pattison, D.R.M., Heaman, J., 2004. Age of the Ballachulish and Glencoe Igneous Complexes (Scottish Highlands), and paragenesis of zircon, monazite and baddeleyite in the Ballachulish Aureole. *J. Geol. Soc. Lond.* **161**, 447–462.

Früh-Green, G.I., Scambelluri, M., Vallis, F., 2001. O-H isotope ratios of high pressure ultramafic rocks: implications for fluid sources and mobility in the subducted hydrous mantle. *Contrib. Mineral. Petrol.* **141**, 145–159.

Fu, B., Touret, J.L.R., Zheng, Y.-F., 2001. Fluid inclusions in coesite-bearing eclogites and jadeite quartzite at Shuanghe, Dabie Shan, China. *J. Metamor. Geol.* **19**, 529–545.

Gebauer, D., Schertl, H.P., Brix, M., Schreyer, W., 1997. 35 Ma old ultrahigh-pressure metamorphism and evidence for very rapid exhumation in the Dora Maira Massif, eastern Alps. *Lithos* **41**, 5–24.

Gray, D.R., Hand, M., Mawby, J., Armstrong, R.A., Miller, J.M., 2004. Sm-Nd and zircon U–Pb ages from garnet-bearing eclogites, NE Oman: constraints on High-P metamorphism. *Earth Planet Sci. Lett.* **222**, 407–422.

Hacker, B.R., Ratschbacher, L., Webb, L., Ireland, T., Walker, D., Dong, S.W., 1998. U/Pb zircon ages constrain the architecture of the ultrahigh-pressure Qinling-Dabie Orogen, China. *Earth Planet Sci. Lett.* **161**, 215–230.

Hacker, B.R., Ratschbacher, L., Webb, L., McWilliams, M.O., Ireland, T., Calvert, A., Dong, S., Wenk, H.-R., Chateigner, D., 2000. Exhumation of ultrahigh-pressure continental crust in east central China: Late Triassic-Early Jurassic tectonic unroofing. *J. Geophys. Res.* **105B**, 13339–13364.

Hermann, J., Rubatto, D., Korsakov, A., 2001. Multiple zircon growth during fast exhumation of diamondiferous, deeply subducted continental crust (Kokchetav Massif, Kazakhstan). *Contrib. Mineral Petrol.* **141**, 66–82.

Hoskin, P.W.O., Black, L.P., 2000. Metamorphic zircon formation by solid-state recrystallization of protolith igneous zircon. *J. Metamor. Geol.* **18**, 423–439.

Iizuka, T., Hirata, T., 2005. Improvements of precision and accuracy in in situ Hf isotope microanalysis of zircon using the laser ablation-MC-ICPMS technique. *Chem. Geol.* **220**, 121–137.

Jahn, B.-m., Rumble, D., Liou, J.G., 2003. Geochemistry and isotope tracer study of UHP metamorphic rocks. In: Carswell, D.A., Compagnoni, R. (Eds.), Ultrahigh Pressure Metamorphism. EMU Notes in Mineralogy, vol. 5, pp. 365–414.

Keay, S., Lister, G., Buick, I., 2001. The timing of partial melting, Barrovian metamorphism and granite intrusion in the Naxos metamorphic core complex, Cyclades, Aegean Sea, Greece. *Tectonophysics* **342**, 275–312.

Kinny, P.D., Maas, R., 2003. Lu–Hf and Sm-Nd isotope systems in zircon. *Rev. Mineral. Geochem.* **53**, 327–341.

Lapen, T.J., Johnson, C.M., Baumgartner, L.P., Mahlen, N.J., Beard, B.L., Amato, J.M., 2003. Burial rates during prograde metamorphism of an ultra-high-pressure terrane: an example from Lago di Cignana, western Alps, Italy. *Earth Planet Sci. Lett.* **215**, 57–72.

Li, X.-P., Zheng, Y.-F., Wu, Y.-B., Chen, F.-K., Gong, B., Li, Y.-L., 2004. Low-T eclogite in the Dabie terrane of China: petrologic and isotopic constraints on fluid activity and radiometric dating. *Contrib. Mineral. Petrol.* **148**, 443–470.

Liati, A., Gebauer, D., 1999. Constraining the prograde and retrograde P-T-t path of Eocene HP rocks by SHRIMP dating difference zircon domain: inferred rated of heating-burial, cooling and exhumation for central Rhodope, northern Greece. *Contrib. Mineral. Petrol.* **135**, 340–354.

Liou, J.G., Zhang, R.-Y., Eide, E.A., Wang, X.M., Ernst, W.G., Maruyama, S., 1996. Metamorphism and tectonics of high-pressure and ultra-high-pressure belts in the Dabie-Sulu region, China. In: Harrison, M.T., Yin, A. (Eds.), *The Tectonics of Asia*. Cambridge University Press, Cambridge, pp. 300–344.

Liu, D.Y., Jian, P., 2004. 243 Ma UHP and 228 Ma retrograde events of the Shuanghe jadeite quartzite, Eastern Dabie Mountains – SHRIMP dating, mineral inclusions and zircon REE patterns. *Acta Geol. Sin. (in Chinese with English abstract)* **78**, 211–217.

Liu, F.L., Xu, Z.Q., 2004. Fluid inclusions hidden in coesite-bearing zircons in ultrahigh-pressure metamorphic rocks from southwestern Sulu terrane in eastern China. *Chinese Sci. Bull.* **49**, 396–404.

Liu, F.L., Xu, Z.Q., Liou, J.G., Song, B., 2004a. SHRIMP U–Pb ages of ultrahigh-pressure and retrograde metamorphism of gneisses, southwest Sulu terrane, eastern China. *J. Metamor. Geol.* **22**, 315–326.

Liu, F.L., Xu, Z.Q., Xue, H.M., 2004b. Tracing the protolith, UHP metamorphism, and exhumation ages of orthogneiss from the SW Sulu terrane (eastern China): SHRIMP U–Pb dating of mineral inclusion-bearing zircons. *Lithos* **78**, 411–429.

Liu, F.L., Yang, J.S., Xu, Z.Q., 2005. Mineral inclusions in zircon domains and geological significance of SHRIMP U–Pb dating for coesite-bearing zircons of paragneiss in Sulu terrane, eastern China. *Sci. China (D)* **48**, 175–184.

Ludwig, K.R., 2001. Users Manual for Isoplot/Ex (rev. 2.49): A Geochronological Toolkit for Microsoft Excel. Berkeley Geochronology Center, Special Publication No. 1a, 55pp.

Mork, M.B.E., Mearns, E.W., 1986. Sm-Nd isotopic systematic of the gabbro-eclogite transition. *Lithos* **19**, 255–267.

Okay, A.I., 1993. Petrology of a diamond and coesite bearing metamorphic terrane: Dabie Shan, China. *Eur. J. Mineral.* **5**, 659–675.

Roberts, M., Finger, F., 1997. Do U–Pb zircon ages from granulites reflect peak metamorphic conditions? *Geology* **25**, 319–322.

Rowley, D.B., Xue, F., Tucker, R.D., Peng, Z.X., Baker, J., Davis, A., 1997. Ages of ultrahigh pressure metamorphism and protolith orthogneisses from the eastern Dabie Shan:U/Pb zircon geochronology. *Earth Planet Sci. Lett.* **151**, 191–203.

Rubatto, D., Gebauer, G., Compagnoni, R., 1999. Dating of eclogite-facies zircons: the age of Alpine metamorphism in the Sesia-Lanzo Zone (Western Alps). *Earth Planet Sci. Lett.* **167**, 141–158.

Rubatto, D., 2002. Zircon trace element geochemistry: partitioning with garnet and the link between U–Pb ages and metamorphism. *Chem. Geol.* **184**, 123–138.

Rubatto, D., Hermann, J., 2003. Zircon formation during fluid circulation in eclogites (Monviso, Western Alps): Implications for Zr and Hf budget in subduction zones. *Geochim. Cosmochim. Acta* **67**, 2173–2187.

Rumble, D., Wang, Q.C., Zhang, R.Y., 2000. Stable isotope geochemistry of marbles from the coesite UHP terrains of Dabieshan and Sulu, China. *Lithos* **52**, 79–95.

Rumble, D., Giorgis, D., Oreland, T., Zhang, Z.-M., Xu, H.-F., Yui, T.-F., Yang, J.-S., Xu, Z.-Q., Liou, J.G., 2002. Low $\delta^{18}O$ zircons, U–Pb dating, and the age of the Qinglongshan oxygen and hydrogen isotope anomaly near Donghai in Jiangsu province, China. *Geochim. Cosmochim. Acta* **66**, 2299–2306.

Rumble, D., Liou, J.G., Jahn, B.-m., 2003. Continental crust subduction and ultrahigh pressure metamorphism. *Treatise Geochem.* **3**, 293–319.

Sassi, R., Harte, B., Carswell, D.A., Han, Y.J., 2000. Trace element distribution in Central Dabie eclogites. *Contrib. Mineral. Petrol.* **139**, 298–315.

Scherer, E., Munker, C., Mezger, K., 2001. Calibration of the lutetium–hafnium clock. *Science* **293**, 683–687.

Schertl, H.P., Okay, A.I., 1994. A coesite inclusion in dolomite in Dabie Shan, China: petrological and rheological significance. *Eur. J. Mineral.* **6**, 995–1000.

Schersten, A., Larson, S.A., Cornell, D.H., Stigh, J., 2004. Ion probe dating of a migmatite in SW Sweden: the fate of zircon in crustal processes. *Precambr. Res.* **130**, 251–266.

Timmermann, H., Stedra, V., Gerdes, A., Noble, S.R., Parrish, R.R., Dorr, W., 2004. The problem of dating high-pressure metamorphism: a U–Pb isotope and geochemical study on eclogites and related rocks of the Marianske Lanze Complex, Czech Republic. *J. Petrol.* **45**, 1311–1338.

Tomaschek, F., Kennedy, A.K., Villa, I.M., Markus, L., Chris, B., 2003. Zircons from Syros, Cyclades, Greece-recrystallization and mobilization of zircon during high-pressure metamorphism. *J. Petrol.* **44**, 1977–2002.

Valley, J.W., Kitchen, N.E., Kohn, M.J., Niendorf, C.R., Spicuzza, M.J., 1995. UWG-2, a garnet standard for oxygen isotope ratio: strategies for high precision and accuracy with laser heating. *Geochim. Cosmochim. Acta* **59**, 5223–5231.

Vavra, G., Gebauer, D., Schmid, R., 1996. Multiple zircon growth and recrystallization during polyphase Late Carboniferous to Triassic metamorphism in granulites of the Ivrea Zone (Southern Alps): an ion microprobe (SHRIMP) study. *Contrib. Mineral Petrol.* **122**, 337–358.

Vavra, G., Schmid, R., Gebauer, D., 1999. Internal morphology, habit and U–Th–Pb microanalysis of amphibole to granulite facies zircon: geochronology of the Ivrea Zone (Southern Alps), Contrib. *Mineral Petrol.* **134**, 380–404.

Vervoort, J.D., Blichert-Toft, J., 1999. Evolution of the depleted mantle: Hf isotope evidence from juvenile rocks through time. *Geochim. Cosmochim. Acta* **63**, 533–556.

Wan, Y.S., Li, R.W., Wilde, S.A., Liu, D.Y., Chen, Z.Y., Yan, L., Song, T.R., Yin, X.Y., 2005. UHP metamorphism and exhumation of the Dabie Orogen, China: evidence from SHRIMP dating of zircon and monazite from a UHP granitic gneiss cobble from the Hefei Basin. *Geochem. Cosmochim. Acta* **69**, 4333–4348.

Wang, X.M., Zhang, R.Y., Liou, J.G., 1995. UHPM terrane in east central China. In: Coleman, R., Wang, X. (Eds.), *Ultrahigh Pressure Metamorphism*. Cambridge University Press, Cambridge, pp. 356–390.

Whitehouse, M.J., Platt, J.P., 2003. Dating high-grade metamorphism-constraints from rare-earth elements in zircons and garnet. *Contrib. Mineral Petrol.* **145**, 61–74.

Wiedenbeck, M., Alle, P., Corfu, F., Griffin, W.L., Meier, M., Oberli, F., von Quadt, A., Roddick, J.C., Spiegel, W., 1995. Three natural zircon standards for U–Th–Pb, Lu–Hf, trace element and REE analyses. *Geostand. Newslett.* **19**, 1–23.

Williams, I.S., Buick, I.S., Cartwright, I., 1996. An extended episode of early Mesoproterozoic metamorphic fluid flow in the Reynolds Range, central Australia. *J. Metamor. Geol.* **14**, 29–47.

Williams, I.S., 1998. U–Th–Pb geochronology by ion microprobe. In: McKibben, M.A., Shanks III, W.C., Ridley, W.I. (Eds.), Applications of Microanalytical Techniques to Understanding Mineralizing Processes. Rev. Econ. Geol. 7, 1–35.

Woodhead, J., Hergta, J., Shelley, M., Egginsb, S., Kemp, R., 2004. Zircon Hf-isotope analysis with an excimer laser, depth profiling, ablation of complex geometries, and concomitant age estimation. *Chem. Geol.* **209**, 121–135.

Wu, Y.-B., Zheng, Y.-F., 2004. Genesis of zircon and its constraints on interpretation of U–Pb age. *Chinese Sci. Bull.* **49**, 1554–1569.

Wu, F.-Y., Yang, Y.H., Xie, L.W., Yang, J.H., Xu, P., 2006. Hf isotopic compositions of the standard zircons and baddeleyites used in U–Pb geochronology. *Chem. Geol.* **232**. doi:10.1016/j.chemgeo.2006.05.003.

Xu, S.-T., Okay, A., Ji, S., Sengor, A.M.C., Su, W., Liu, Y., Jiang, L., 1992. Diamond from the Dabie Shan metamorphic rocks and its implication for the tectonic setting. *Science* **256**, 80–82.

Xu, S.-T., Liu, Y.-C., Chen, G.-B., Compagnoni, R., Rolfo, F., He, M.-C., Liu, H.-F., 2003. New finding of micro-diamonds in eclogites from the Dabie-Sulu region in east-central China. *Chinese Sci. Bull.* **48**, 988–994.

Xu, P., Wu, F.-Y., Xie, L.-W., Yang, Y.-H., 2004. Hf isotopic compositions of the standard zircons for U–Pb dating. *Chinese Sci. Bull.* **49**, 1642–1648.

Xu, S.-T., Liu, Y.-C., Chen, G.-B., Ji, S.-Y., Ni, P., Xiao, W.-S., 2005. Microdiamonds, their classification and tectonic implications for the host eclogites from the Dabie and Su-Lu regions in central eastern China. *Mineral. Mag.* **69**, 509–520.

Yang, J.S., Wooden, J.L., Wu, C.L., Liu, F.L., Xu, Z.Q., Shi, R.D., Katayama, I., Liou, J.G., Maruyama, S., 2003. SHRIMP U–Pb dating of coesite-bearing zircon from the ultrahigh-pressure metamorphic rocks, Sulu terrane, east China. *J. Metamor. Geol.* **21**, 551–560.

Yuan, H.L., Gao, S., Liu, X.M., Li, H.M., Gunther, D., Wu, F.Y., 2004. Accurate U–Pb age and trace element determinations of zircon by laser ablation-inductively coupled plasma mass spectrometry. *Geostand. Newsl.* **28**, 353–370.

Zhang, R.Y., Liou, J.G., 1996. Coesite inclusions in dolomite from eclogite in the southern Dabie Mtns, China: the significance of carbonate minerals in UHPM rocks. *Am. Mineral.* **81**, 181–186.

Zhang, R.Y., Liou, J.G., Zheng, Y.-F., Fu, B., 2003. Transition of UHP eclogites to gneissic rocks of low-amphibolite facies during exhumation: evidence from the Dabie terrane, central China. *Lithos* **70**, 269–291.

Zhang, R.Y., Yang, J.S., Wooden, J.L., Liou, J.G., Li, T.F., 2005. U–Pb SHRIMP geochronology of zircon in garnet peridotite from the Sulu UHP terrane, China: Implications for mantle metasomatism and subduction-zone UHP metamorphism. *Earth Planet Sci. Lett.* **237**, 729–743.

Zhao, Z.-F., Zheng, Y.-F., Wei, C.-S., Wu, Y.-B., 2004. Zircon isotope evidence for recycling of subducted continental crust in post-collisional granitoids from the Dabie terrane in China. *Geophys. Res. Lett.* **31**, L22602. doi:10.1029/2004GL02106.

Zhao, Z.-F., Zheng, Y.-F., Wei, C.-S., Wu, Y.-B., Chen, F.-K., Jahn, B.-M., 2005. Zircon U–Pb age, element and C–O isotope geochemistry of post-collisional mafic-ultramafic rocks from the Dabie orogen in east-central China. *Lithos* **83**, 1–28.

Zheng, Y.-F., 1993a. Calculation of oxygen isotope fractionation in anhydrous silicate minerals. *Geochim. Cosmochim. Acta* **57**, 1079–1091.

Zheng, Y.-F., 1993b. Calculation of oxygen isotope fractionation in hydroxyl-bearing silicates. *Earth Planet Sci. Lett.* **120**, 247–263.

Zheng, Y.-F., Fu, B., Gong, B., Wang, Z.-R., 1998a. Carbon isotope anomaly in marbles associated with eclogites from the Dabie Mountains in China. *J. Geol.* **106**, 97–104.

Zheng, Y.-F., Fu, B., Li, Y.-L., Xiao, Y.-L., Li, S.-G., 1998b. Oxygen and hydrogen isotope geochemistry of ultrahigh pressure eclogites from the Dabie Mountains and the Sulu terrane. *Earth Planet Sci. Lett.* **155**, 113–129.

Zheng, Y.-F., Fu, B., Xiao, Y.-L., Li, Y.-L., Gong, B., 1999. Hydrogen and oxygen isotope evidence for fluid-rock interactions in the stages of pre- and post-UHP metamorphism in the Dabie Mountains. *Lithos* **46**, 677–693.

Zheng, Y.-F., Wang, Z.-R., Li, S.-G., Gong, B., 2002. Oxygen isotope equilibrium between eclogite minerals and its constraints on mineral Sm-Nd chronometer. *Geochim. Cosmochim. Acta* **66**, 625–634.

Zheng, Y.-F., Fu, B., Gong, B., Li, L., 2003. Stable isotope geochemistry of ultrahigh pressure metamorphic rocks from the Dabie-Sulu orogen in China: Implications for geodynamics and fluid regime. *Earth Sci. Rev.* **62**, 105–161.

Zheng, Y.-F., Wu, Y.-B., Chen, F.-K., Gong, B., Zhao, Z.-F., 2004. Zircon U–Pb and oxygen isotope evidence for a large-scale ^{18}O depletion event in igneous rocks during the Neoproterozoic. *Geochim. Cosmochim. Acta* **68**, 4145–4165.

Zheng, Y.-F., Wu, Y.-B., Zhao, Z.-F., Zhang, S.-B., Xu, P., Wu, F.-Y., 2005a. Metamorphic effect on zircon Lu–Hf and U–Pb isotope systems in ultrahigh-pressure metagranite and metabasite. *Earth Planet Sci. Lett.* **240**, 378–400.

Zheng, Y.-F., Zhou, J.-B., Wu, Y.-B., Xie, Z., 2005b. Low-grade metamorphic rocks in the dabie-sulu orogenic belt: a passive-margin accretionary wedge deformed during continent subduction. *Intern. Geol. Rev.* **47**, 851–871.

Zheng, Y.-F., Zhao, Z.-F., Wu, Y.-B., Zhang, S.-B., Liu, X.M., Wu, F.-Y., 2006. Zircon U–Pb age, Hf and O isotope constraints on protolith origin of ultrahigh-pressure eclogite and gneiss in the Dabie orogen. *Chem. Geol.* **231**, 135–158.